B meson decay anomaly with a nonuniversal $U(1)'$ extension

R. Martinez,* F. Ochoa,† and J. M. Quimbayo‡
Departamento de Física, Universidad Nacional de Colombia, Ciudad Universitaria, K. 45 No. 26-85, Bogotá D.C., Colombia

(Received 10 January 2018; published 27 August 2018)

We propose an extension of the standard model with an extra $U(1)'$ Abelian symmetry, three Higgs doublets and two Higgs singlets, where the new $U(1)'$ charges are flavor nonuniversal. As a result, the model introduces an enlarger particle spectrum in the TeV scale with large new physics possibilities. The model reproduces the mixing angles and mass structures of the quarks, charged and neutral leptons. We found scenarios where the observed anomaly of the $B^+ \to K^+\ell\ell$ decay can be explained due to the existence of couplings with new extra fermions at the TeV scale. By modifying the parametrization of the mixing matrices, we found solution in the decoupling limit.

DOI: 10.1103/PhysRevD.98.035036

I. INTRODUCTION

Despite all its success, the standard model (SM) of Glashow, Weinberg, and Salam [1] does not account for all the theoretical and experimental observations; therefore it is believed that there is a more fundamental theory where the SM emerges as an effective lower limit at the electroweak scale. For example, the fermion mass hierarchy and the neutrino mass problem are two related subjects that may be understood as manifestations of an underlying theory beyond the SM [2,3]. Also, there are some observables that show some tensions from the SM predictions, which may be associated to new physics. Among the different observations accessible to collider physics, the flavor observables imposes stringent limits to many SM extensions. In particular, the lepton universality exhibited by the SM is sensitive to new physics that can be tested in rare semileptonic transitions of mesons [4–6]. Recently, the ratio of the branching fractions of B meson decays into muon and electron pairs was reported by the LHCb collaboration [7], where a deviation from the SM prediction within 2.6σ suggest us a possible lepton universality violation not explained in the framework of the SM.

From the theoretical point of view, the mass hierarchy problem can be addressed in a model independent approach by assuming texture zero structures for the mass matrices [8]. Relations between mixing angles and masses can be also derived for both quarks and lepton sectors in models with broken flavor symmetries. These symmetries, that relates the three fermion families in a nontrivial way, have been extensively studied in the literature in different extensions of the SM, either as a continuous Abelian or non-Abelian extensions [9], or as a discrete flavor symmetry [10]. On the other hand, many grand unified and superstring models predicts one or multiple extra Abelian symmetries in their effective low energy limit [11], which motivates extensions of the SM with an extra U(1)' gauge symmetry. If this symmetry is family nonuniversal, it is possible to connect the flavor problem with the group properties of these models. Also, these type of extensions imply a new extra neutral Z' boson which, in the framework of a nonuniversal model, produces new contributions to flavor-changing neutral current (FCNC) processes. Although these type of interactions are strongly suppressed in the SM, which is consistent with most of the experimental observations, there are some anomalies reported, as the aforementioned decay $B^+ \to K^+\ell^+\ell^-$, corresponding to a $b \to s$ FCNC process.

Motivated initially by the mass hierarchy of the quarks, in the $U(1)'$ model proposed in Ref. [12], the new Abelian charge distinguishes one family of quarks from the other two, and newly vectorlike quarks are introduced in order to restore the cancellation of the chiral anomalies. This model is universal in the lepton sector. A modification of the above model was presented in [13], where newly charged leptons are also introduced in order to obtain nonuniversal lepton families compatible with the cancellation of the chiral anomalies. The above structure can reproduce the elements of the mixing mass matrix and the squared-mass diferences data from neutrinos oscillations experiments.

In this article, we combine the nonuniversal $U(1)'$ model from [13] with a three Higgs doublet model in order to explain the anomaly measured by the LHCb in the ratio of the branching fractions of $B^+ \to K^+\mu^+\mu^-$ to $B^+ \to K^+e^+e^-$ decays. This model was already presented

*remartinezm@unal.edu.co
†faochoap@unal.edu.co
‡jmquimbayog@unal.edu.co

in [14], where the three doublets may induce naturally the fermion hierarchy, while the smallness of the neutrinos can be implemented through an inverse see saw mechanism, where the vacuum expectation value that breaks the extra $U(1)'$ symmetry defines the large mass scale.

II. SURVEY OF THE MODEL

A. Particle content

The model is an extension of the SM group, with the addition of a nonuniversal Abelian gauge symmetry [which we denote as $\mathrm{U}(1)_X$] whose gauge boson and coupling constant are Z'_μ and g_X, respectively, while the weak hypercharge is defined as usual through the Gell-Mann-Nishijima relation:

$$Q = I_3 + \frac{Y}{2}, \tag{1}$$

with Q the electric charge operator and I_3 the isospin.

The additional gauge symmetry introduces new chiral anomaly equations which can be solved by assigning nontrivial X-quantum numbers to the fermions of the SM [12]. If this new $U(1)$ charges are different from the SM $U(1)_Y$ charges, then anomaly cancellation require new quarks and leptons to be added into the spectrum with masses at a larger scale than the electroweak scale [15]. For simplicity, all the new particles are assumed to be singlets under the gauge $SU(2)_L$ group. In order to provide masses to the new sector, we introduce a neutral Higgs singlet χ with nonvanishing VEV, and $\mathrm{U}(1)_X$ charge $X = -1/3$ in such a way that it spontaneously breaks the new gauge symmetry. Another scalar singlet σ identical to χ but without VEV is introduced, which can play the role of a dark matter candidate, such as in the $U(1)'$ extension in [16].

On the other hand, the phenomenological fermions define three mass scales. First, the top quark (t) is the heaviest observed femion at 10^2 GeV scale. Second, the tau lepton and bottom quark (τ, b) are in the 10^0 GeV scale. Finally, the muon and strange quark (μ, s) are in the 10^2 MeV scale. This general structure can be directly induced with three Higgs doublets with vacuum expectation values (VEV) $v_1 > v_2 > v_3$ associated to the three scales above. The chosen particle spectrum is presented in the Table I where three new quarks ($\mathcal{T}$, $\mathcal{J}^{1,2}$) and two charged leptons ($\mathcal{E}^{1,2}$) are introduced. To obtain masses for the active neutrinos, we introduce three right-handed neutrinos $\nu_R^{1,2,3}$ with nontrivial $U(1)_X$ charges, which allow the coupling with the ordinary lepton doublets ℓ_L, but because of their X-charge, they do not generate Majorana mass terms. The addition of Majorana fermions, $\mathcal{N}_R^{1,2,3}$, allow an inverse seesaw mechanism in order to explain the smallness of the active neutrinos.

In order to obtain predictable and analytical relations for the masses and mixing angles of the fermions according to observations, we assign specific $\mathbb{Z}_2$ symmetry parities, which are shown as superscripts in the X-charges. It is to note that, despite the scalar doublets Φ_2 and Φ_3 have the same X charge, they have opposite $\mathbb{Z}_2$ parity such that their couplings to fermions are complementary.

TABLE I. Nonuniversal X quantum number and $\mathbb{Z}_2$ parity for SM and non-SM fermions.

Bosons	$X^{\pm}$	Quarks	$X^{\pm}$	Leptons	$X^{\pm}$
Scalar Doublets		SM Fermionic Doublets			
$\Phi_1 = \begin{pmatrix} \phi_1^+ \\ \frac{h_1+v_1+i\eta_1}{\sqrt{2}} \end{pmatrix}$	$\frac{+2}{3}^+$	$q_L^1 = \begin{pmatrix} u^1 \\ d^1 \end{pmatrix}_L$	$\frac{+1}{3}^+$	$\ell_L^e = \begin{pmatrix} \nu^e \\ e^e \end{pmatrix}_L$	0^+
$\Phi_2 = \begin{pmatrix} \phi_2^+ \\ \frac{h_2+v_2+i\eta_2}{\sqrt{2}} \end{pmatrix}$	$\frac{+1}{3}^-$	$q_L^2 = \begin{pmatrix} u^2 \\ d^2 \end{pmatrix}_L$	0^-	$\ell_L^\mu = \begin{pmatrix} \nu^\mu \\ e^\mu \end{pmatrix}_L$	0^+
$\Phi_3 = \begin{pmatrix} \phi_3^+ \\ \frac{h_3+v_3+i\eta_3}{\sqrt{2}} \end{pmatrix}$	$\frac{+1}{3}^+$	$q_L^3 = \begin{pmatrix} u^3 \\ d^3 \end{pmatrix}_L$	0^+	$\ell_L^\tau = \begin{pmatrix} \nu^\tau \\ e^\tau \end{pmatrix}_L$	-1^+
Scalar Singlets		SM Fermionic Singlets			
$\chi = \frac{\xi_\chi+v_\chi+i\zeta_\chi}{\sqrt{2}}$	$\frac{-1}{3}^+$	$u_R^{1,3}$	$\frac{+2}{3}^+$	e_R^e	$\frac{-4}{3}^+$
σ	$\frac{-1}{3}^-$	u_R^2	$\frac{+2}{3}^-$	e_R^μ	$\frac{-1}{3}^+$
		$d_R^{1,2,3}$	$\frac{-1}{3}^-$	e_R^τ	$\frac{-4}{3}^-$
Gauge bosons		Non-SM Quarks		Non-SM Leptons	
$W_\mu^\pm$	0^+	$\mathcal{T}_L$	$\frac{+1}{3}^-$	$\nu_R^{1,2,3}$	$\frac{+1}{3}^+$
W_μ^3	0^+	$\mathcal{T}_R$	$\frac{+2}{3}^-$	$\mathcal{N}_R^{1,2,3}$	0^+
B_μ	0^+	$\mathcal{J}_L^{1,2}$	0^+	$\mathcal{E}_L^1, \mathcal{E}_R^2$	-1^+
Z'_μ	0^+	$\mathcal{J}_R^{1,2}$	$\frac{-1}{3}^+$	$\mathcal{E}_R^1, \mathcal{E}_L^2$	$\frac{-2}{3}^+$

Finally, since the new fermions are vectorlike under the SM group, they do not introduce any extra $SU(2)_L \times U(1)_Y$ contribution to the anomaly equations. However, the symmetry $U(1)_X$ may generate the following pure and mixed anomalies:

$$\begin{aligned}
[U(1)_X]^3 \to A_1 &= \sum_{\ell,Q}[X_{\ell_L}^3 + 3X_{Q_L}^3] - \sum_{\ell,Q}[X_{\ell_R}^3 + 3X_{Q_R}^3] \\
[SU(3)_c]^2 U(1)_X \to A_2 &= \sum_{Q} X_{Q_L} - \sum_{Q} X_{Q_R} \\
[SU(2)_L]^2 U(1)_X \to A_3 &= \sum_{\ell} X_{\ell_L} + 3\sum_{Q} X_{Q_L}, \\
[U(1)_Y]^2 U(1)_X \to A_4 &= \sum_{\ell,Q}[Y_{\ell_L}^2 X_{\ell_L} + 3Y_{Q_L}^2 X_{Q_L}] - \sum_{\ell,Q}[Y_{\ell_R}^2 X_{\ell_R} + 3Y_{Q_R}^2 X_{Q_R}] \\
U(1)_Y [U(1)_X]^2 \to A_5 &= \sum_{\ell,Q}[Y_{\ell_L} X_{\ell_L}^2 + 3Y_{Q_L} X_{Q_L}^2] - \sum_{\ell,Q}[Y_{\ell_R} X_{\ell_R}^2 + 3Y_{Q_R} X_{Q_R}^2] \\
[\mathrm{Grav}]^2 \otimes U(1)_X \to A_6 &= \sum_{\ell,Q}[X_{\ell_L} + 3X_{Q_L}] - \sum_{\ell,Q}[X_{\ell_R} + 3X_{Q_R}]
\end{aligned} \tag{2}$$

where the sums in Q runs over all the quarks, and ℓ over all leptons. However, by direct calculation, it is possible to verify that the chosen $U(1)_X$ charges satisfy the cancellation of the anomalies in (2), so that the model is free from chiral anomalies.

B. Lagrangians

1. Yukawa interactions

The most general Yukawa Lagrangian must obey the gauge symmetry $G_{\rm SM}\times U(1)_X$ in order to obtain a renomarlizable model, where $G_{\rm SM}$ is the SM gauge group. However, we impose additionaly that the interactions respect the discrete Z_2 symmetry, where each particle has the intrisic Z_2-parity shown in Table I. Since there are particles with different Z_2-parities, not all couplings between fermions and scalars are allowed. Specifically, the Yukawa Lagrangian allowed by the symmetries of the model for the up- and down-like quarks are

$$\begin{aligned}-\mathcal{L}_U &= h^{11}_{3u}\overline{q^1_L}\tilde{\Phi}_3 u^1_R + h^{12}_{2u}\overline{q^1_L}\tilde{\Phi}_2 u^2_R + h^{13}_{3u}\overline{q^1_L}\tilde{\Phi}_3 u^3_R + h^{22}_{1u}\overline{q^2_L}\tilde{\Phi}_1 u^2_R + h^{31}_{1u}\overline{q^3_L}\tilde{\Phi}_1 u^1_R + h^{33}_{1u}\overline{q^3_L}\tilde{\Phi}_1 u^3_R \\ &+ h^1_{2\mathcal{T}}\overline{q^1_L}\tilde{\Phi}_2\mathcal{T}_R + h^2_{1\mathcal{T}}\overline{q^2_L}\tilde{\Phi}_1\mathcal{T}_R + g^1_{\sigma u}\overline{\mathcal{T}_L}\sigma u^1_R + g^2_{\chi u}\overline{\mathcal{T}_L}\chi u^2_R + g^3_{\sigma u}\overline{\mathcal{T}_L}\sigma u^3_R + g_{\chi\mathcal{T}}\overline{\mathcal{T}_L}\chi\mathcal{T}_R + \text{H.c.}, \end{aligned} \tag{3}$$

$$\begin{aligned}-\mathcal{L}_D &= h^{11}_{1\mathcal{J}}\overline{q^1_L}\Phi_1\mathcal{J}^1_R + h^{21}_{2\mathcal{J}}\overline{q^2_L}\Phi_2\mathcal{J}^1_R + h^{31}_{3\mathcal{J}}\overline{q^3_L}\Phi_3\mathcal{J}^1_R + h^{12}_{1\mathcal{J}}\overline{q^1_L}\Phi_1\mathcal{J}^2_R + h^{22}_{2\mathcal{J}}\overline{q^2_L}\Phi_2\mathcal{J}^2_R + h^{32}_{3\mathcal{J}}\overline{q^3_L}\Phi_3\mathcal{J}^2_R \\ &+ h^{21}_{3d}\overline{q^2_L}\Phi_3 d^1_R + h^{22}_{3d}\overline{q^2_L}\Phi_3 d^2_R + h^{23}_{3d}\overline{q^2_L}\Phi_3 d^3_R + h^{31}_{2d}\overline{q^3_L}\Phi_2 d^1_R + h^{32}_{2d}\overline{q^3_L}\Phi_2 d^2_R + h^{33}_{2d}\overline{q^3_L}\Phi_2 d^3_R \\ &+ g^{11}_{\sigma d}\overline{\mathcal{J}^1_L}\sigma^* d^1_R + g^{11}_{\sigma d}\overline{\mathcal{J}^1_L}\sigma^* d^2_R + g^{13}_{\sigma d}\overline{\mathcal{J}^1_L}\sigma^* d^3_R + g^{21}_{\sigma d}\overline{\mathcal{J}^2_L}\sigma^* d^1_R + g^{22}_{\sigma d}\overline{\mathcal{J}^2_L}\sigma^* d^2_R + g^{23}_{\sigma d}\overline{\mathcal{J}^2_L}\sigma^* d^3_R + g^1_{\chi\mathcal{J}}\overline{\mathcal{J}^1_L}\chi^*\mathcal{J}^1_R \\ &+ g^2_{\chi\mathcal{J}}\overline{\mathcal{J}^2_L}\chi^*\mathcal{J}^2_R + \text{H.c.}, \end{aligned} \tag{4}$$

while for the neutral and charged leptons we obtain:

$$\begin{aligned}-\mathcal{L}_N &= h^{ee}_{3\nu}\overline{\ell^e_L}\tilde{\Phi}_3\nu^1_R + h^{e\mu}_{3\nu}\overline{\ell^e_L}\tilde{\Phi}_3\nu^2_R + h^{e\tau}_{3\nu}\overline{\ell^e_L}\tilde{\Phi}_3\nu^3_R + h^{\mu e}_{3\nu}\overline{\ell^\mu_L}\tilde{\Phi}_3\nu^1_R + h^{\mu\mu}_{3\nu}\overline{\ell^\mu_L}\tilde{\Phi}_3\nu^2_R + h^{\mu\tau}_{3\nu}\overline{\ell^\mu_L}\tilde{\Phi}_3\nu^3_R + g^{ij}_{\chi\mathcal{N}}\overline{\nu^{iC}_R}\chi^*\mathcal{N}^j_R \\ &+ \frac{1}{2}\overline{\mathcal{N}^{iC}_R}M^{ij}_{\mathcal{N}}\mathcal{N}^j_R + \text{H.c.}, \end{aligned} \tag{5}$$

$$\begin{aligned}-\mathcal{L}_E &= h^{e\mu}_{3e}\overline{\ell^e_L}\Phi_3 e^\mu_R + h^{\mu\mu}_{3e}\overline{\ell^\mu_L}\Phi_3 e^\mu_R + h^{\tau e}_{2e}\overline{\ell^\tau_L}\Phi_3 e^e_R + h^{\tau\tau}_{2e}\overline{\ell^\tau_L}\Phi_2 e^\tau_R + h^{e1}_{1E}\overline{\ell^e_L}\Phi_1\mathcal{E}^1_R + h^{\mu 1}_{1\mathcal{E}}\overline{\ell^\mu_L}\Phi_1\mathcal{E}^1_R + g^{1e}_{\chi e}\overline{\mathcal{E}^1_L}\chi^* e^e_R + g^{2\mu}_{\chi e}\overline{\mathcal{E}^2_L}\chi e^\mu_R \\ &+ g^1_{\chi\mathcal{E}}\overline{\mathcal{E}^1_L}\chi\mathcal{E}^1_R + g^2_{\chi\mathcal{E}}\overline{\mathcal{E}^2_L}\chi^*\mathcal{E}^2_R + \text{H.c.}, \end{aligned} \tag{6}$$

where $\tilde{\Phi} = i\sigma_2\Phi^*$ are the scalar doublet conjugates and the Majorana mass components are denoted as $M^{ij}_{\mathcal{N}}$.

2. Gauge and scalar boson interactions

The Higgs kinetic Lagrangian contains the couplings among vector gauge and scalar bosons, which takes the general form

$$\mathcal{L}_{\rm kin} = (D_\mu S)^\dagger (D^\mu S), \tag{7}$$

where the covariant derivative is defined as:

$$D^\mu = \partial^\mu - igW^\mu_\alpha T^\alpha_S - ig'\frac{Y_S}{2}B^\mu - ig_X X_S Z'^\mu. \tag{8}$$

The parameters $2T^\alpha_S$ corresponds to the Pauli matrices when $S=\Phi_{1,2,3}$ and $T^\alpha_S = 0$ when $S=\chi$, σ, while Y_S and X_S correspond to the hypercharge and $U(1)_X$ charge according to the values in table I. The gauge coupling constants g and g' obey the same relation as in the SM, $g' = g\tan\theta_W$, with θ_W the Weinberg angle.

3. Dirac Lagrangian

Finally, the interactions of fermions through vector gauge fields are described by the following Lagrangian:

$$\mathcal{L}_D = i\overline{f_{Li}}\gamma^\mu D_\mu f_{Li} + i\overline{f_{Ri}}\gamma^\mu D_\mu f_{Ri}, \tag{9}$$

where f_i runs over all flavor of fermions, and, as usual, a sum over repeated indices is implied. The covariant derivative D^μ is similar to (8) but changing the scalar parameters by the corresponding fermion parameters.

C. Mass eigenstates and interactions

1. Fermion masses

The Yukawa Lagrangians from (3) to (6) provide masses to all the fermions after the symmetries of the model breaks spontaneously, through the vacuum structure of the Higgs

fields shown in Table I. In general, the mass terms have the following form:

$$-\mathcal{L}_f = \overline{\mathbf{f}_L} M_f \mathbf{f}_R + \text{H.c.}, \tag{10}$$

where $\mathbf{f}$ are fermion multiplets with components of the same electric charge, namely

$$\begin{aligned} \mathbf{f}:\ \mathbf{U} &= (u^1, u^2, u^3, \mathcal{T}) \\ \mathbf{D} &= (d^1, d^2, d^3, \mathcal{J}^1, \mathcal{J}^2) \\ \mathbf{E} &= (e^e, e^\mu, e^\tau, \mathcal{E}^1, \mathcal{E}^2) \\ \mathbf{N}_L &= (\nu_L^{e,\mu,\tau}, \nu_R^{1,2,3C}, \mathcal{N}_R^{1,2,3C}), \end{aligned} \tag{11}$$

and M_f are complex nondiagonal mass matrices. In general, the above mass matrices can be diagonalized by biunitary transformations of the form:

$$m_f = (V_L^f)^\dagger M_f V_R^f, \tag{12}$$

which, after replacing in (10), lead us to the left- and right-handed mass basis:

$$\tilde{\mathbf{f}}_L = (V_L^f)^\dagger \mathbf{f}_L, \qquad \tilde{\mathbf{f}}_R = (V_R^f)^\dagger \mathbf{f}_R, \tag{13}$$

where:

$$\begin{aligned} \tilde{\mathbf{f}}:\ \tilde{\mathbf{U}} &= (u, c, t, T) \\ \tilde{\mathbf{D}} &= (d, s, b, J^1, J^2) \\ \tilde{\mathbf{E}} &= (e, \mu, \tau, E^1, E^2) \\ \tilde{\mathbf{N}}_L &= (\nu_L^{1,2,3}, \tilde{\nu}_R^{1,2,3C}, N_R^{1,2,3C}), \end{aligned} \tag{14}$$

The specific form of the matrices $V_{L,R}^f$ depends on the Yukawa structure of the original Lagrangians in (3)–(6). In particular, with the choosen Z_2-parities, these Yukawa terms lead us to predictible mass structures for quarks, charged leptons and neutrinos, as shown in [14], which we summarize in the Appendix B.

2. The unitary constraint

Each rotation matrix in (13) must obey the unitary condition

$$(V_{L,R}^f)^\dagger V_{L,R}^f = I, \tag{15}$$

where I is the identity. In the above relation, we must take into account that the sum from the matrix products contain two contributions due to the components with ordinary SM particles and the newly vectorlike fermions. Labeling $a, b, c, \ldots$ the components with ordinary femions, and $\alpha, \beta, \gamma, \ldots$ the exotic ones, the unitary condition in (15) can be written in tensor form as

$$\begin{aligned} \delta_{ij} &= (V_{L,R}^*)_{ij}(V_{L,R})_{jk} \\ &= (V_{L,R}^*)_{ia}(V_{L,R})_{ak} + (V_{L,R}^*)_{i\alpha}(V_{L,R})_{\alpha k}. \end{aligned} \tag{16}$$

In particular, for the SM components:

$$\delta_{cb} = (V_{L,R}^*)_{ca}(V_{L,R})_{ab} + (V_{L,R}^*)_{c\alpha}(V_{L,R})_{\alpha b}. \tag{17}$$

Thus, the pure SM submatrix $(V_{L,R})_{ab}$ does not satisfy an exact unitary relation, but it is deviated by a small contribution due to new physics from the extra particle content. The relation (17) is conveniently written as:

$$(V_{L,R}^*)_{ca}(V_{L,R})_{ab} = \delta_{cb} - (V_{L,R}^*)_{c\alpha}(V_{L,R})_{\alpha b}. \tag{18}$$

3. Gauge bosons

After the symmetry breaking, we obtain from the kinetic Lagrangian in (7) the charged mass eigenstates

$$W_\mu^\pm = \frac{1}{\sqrt{2}}(W_\mu^1 \mp W_\mu^2), \tag{19}$$

with squared mass $M_\pm^2 = g^2 v^2/4$, where the electroweak vacuum expectation value $v = 246$ GeV is defined with the VEV of each scalar doublet as

$$v = \sqrt{v_1^2 + v_2^2 + v_3^2}. \tag{20}$$

As for the neutral gauge sector, we obtain in the basis (W_μ^3, B_μ, Z_μ') the following symmetric squared mass matrix:

$$\begin{aligned} M_0^2 &= \frac{g^2}{4}\begin{pmatrix} v^2 & -T_W v^2 & | & -\frac{2g_X}{3g}(v^2 + v_1^2) \\ * & T_W^2 v^2 & | & \frac{2g_X}{3g} T_W (v^2 + v_1^2) \\ - & - & - & - \\ * & * & | & \frac{4g_X^2}{9g^2}(v_\chi^2 + v^2 + 3v_1^2) \end{pmatrix} \\ &= \begin{pmatrix} A & | & C \\ - & - & - \\ C^T & | & D \end{pmatrix}, \end{aligned} \tag{21}$$

where $T_W = \tan\theta_W$ is the tangent of the Weinberg angle. Taking into account the hierarchy $v_\chi \gg v$, the above mass matrix can be diagonalized analytically by the recursive expansion method [17]. First, according to the block diagonalization shown in Appendix A, we can reduce the above 3×3 mass matrix into one 2×2 mass matrix and a heavy mass associated to the Z' boson:

$$a \approx A - CD^{-1}C^T = N\begin{pmatrix} 1 & -T_W \\ -T_W & T_W^2 \end{pmatrix},$$
$$b \approx D = \frac{g_X^2}{9}(v_\chi^2 + v^2 + 3v_1^2), \tag{22}$$

where $N = \frac{1}{4}(v^2 - \frac{(v^2+v_1^2)^2}{v_\chi^2})$, while the transformation matrix that induces the above block diagonalization is:

$$V = \begin{pmatrix} I & F \\ -F^T & I \end{pmatrix} = \begin{pmatrix} 1 & 0 & -S_\theta C_W \\ 0 & 1 & S_\theta S_W \\ S_\theta C_W & -S_\theta S_W & 1 \end{pmatrix}, \tag{23}$$

where the sine of the mixing angle θ has been defined as

$$S_\theta = \frac{3}{2}\left(\frac{v^2 + v_1^2}{v_\chi^2}\right)\frac{g}{g_X}. \tag{24}$$

We clarify that in general an additional $Z - Z'$ mixing angle results from the gauge kinetic terms, which can be neglected at a higher scale. This mixing may also arise due to radiative corrections. However, any $Z - Z'$ mixing arisen in the model is very restricted by the LEP data, limiting S_θ to small values. In Ref. [16] the deviations on the Z pole observables due to the mixing angle were evaluated in a $U(1)_X$ model with the same gauge couplings as here, showing allowed mixing angle of the order up to 10^{-4}

Second, the submatrix a in (22) has the following mass eigenvalues:

$$m_A^2 = 0, \qquad m_Z^2 = \frac{g^2}{C_W^2}N, \tag{25}$$

while the associated rotation matrix is

$$p = \begin{pmatrix} S_W & C_W \\ C_W & -S_W \end{pmatrix}. \tag{26}$$

The total rotation into mass eigenstates is the combination of the rotations (23) and (26),

$$R_0 = PV = \begin{pmatrix} p & 0 \\ 0 & 1 \end{pmatrix}V = \begin{pmatrix} S_W & C_W & 0 \\ C_W & -S_W & S_\theta \\ -S_\theta C_W & S_\theta S_W & 1 \end{pmatrix}, \tag{27}$$

obtaining the mass eigenstates:

$$\tilde{V}_\mu = R_0 V_\mu \Rightarrow \begin{pmatrix} A_\mu \\ Z_{1\mu} \\ Z_{2\mu} \end{pmatrix} = R_0 \begin{pmatrix} W_\mu^3 \\ B_\mu \\ Z'_\mu \end{pmatrix}, \tag{28}$$

where A_μ is identified with the photon. We see that in the limit $S_\theta = 0$, we obtain $Z_1 = Z = C_W W^3 - S_W B$ and $Z_2 = Z'$, with Z the SM neutral gauge boson.

4. Neutral currents

The weak interaction of fermions is contained into the Dirac Lagrangian in (9). First, taking into account the mass eigenstates in (19) and (28), the covariant derivative become

$$D^\mu = \partial^\mu - ig(W^{\mu+}T_f^- + W^{\mu-}T_f^+) - \tilde{V}_m^\mu\left[ig(R_0^T)_{1m}T_f^3 + ig'\frac{Y_f}{2}(R_0^T)_{2m} + ig_X X_f (R_0^T)_{3m}\right], \tag{29}$$

where $2T_f^\pm$ is the combination $(\sigma_1 \pm \sigma_2)$ between the first two Pauli matrices and $2T_f^3$ the third Pauli matrix for fermion fields f doublets of $SU(2)$, while $2T_f^\pm = 2T_f^3 = 0$ when f are singlets. The terms $(R_0^T)_{nm}$ correspond to the components of the transpose rotation matrix between the neutral weak and mass eigenstates, as defined in (27), and $\tilde{V}_m^\mu$ the corresponding neutral gauge bosons in mass eigenstate, where $(\tilde{V}_1^\mu, \tilde{V}_2^\mu, \tilde{V}_3^\mu) = (A^\mu, Z_1^\mu, Z_2^\mu)$. Applying the above covariant derivative into the Dirac Lagrangian (9), we obtain the following neutral gauge interactions:

$$\mathcal{L}_{NC} = \frac{g}{2}[\overline{f_{Li}}\gamma_\mu \tilde{V}_m^\mu g_{Lm}^{(f_i)} f_{Li} + \overline{f_{Ri}}\gamma_\mu \tilde{V}_m^\mu g_{Rm}^{(f_i)} f_{Ri}], \tag{30}$$

where $g_{L,Rm}^{(f_i)}$ are the electroweak neutral current couplings, defined in general as:

$$g_m^{(f)} = \pm(R_0^T)_{1m} + T_W Y_f (R_0^T)_{2m} + \frac{2g_X}{g}X_f(R_0^T)_{3m}, \tag{31}$$

for fermions in doublet representations, where the $\pm$ sign is associated to the upper or lower component of the doublet, and

$$g_m^{(f)} = T_W Y_f (R_0^T)_{2m} + \frac{2g_X}{g}X_f(R_0^T)_{3m}, \tag{32}$$

for singlets. In particular, for the ordinary SM fermions, labeled with the index a, the left-handed couplings are

$$g_{L1}^{(f_a)} = 2Q_{f_a}S_W,$$
$$g_{L2}^{(f_a)} = \frac{1}{C_W}(I_3 - 2Q_{f_a}S_W^2) + 2X_{f_{La}}\frac{g_X}{g}S_\theta,$$
$$g_{L3}^{(f_a)} = \frac{1}{C_W}(-I_3 + 2Q_{f_a}S_W^2)S_\theta + 2X_{f_{La}}\frac{g_X}{g}, \tag{33}$$

and for right-handed fermions

$$g_{R1}^{(f_a)} = 2Q_{f_a}S_W,$$
$$g_{R2}^{(f_a)} = -2Q_{f_a}\frac{S_W^2}{C_W} + 2X_{f_{Ra}}\frac{g_X}{g}S_\theta,$$
$$g_{R3}^{(f_a)} = 2Q_{f_a}\frac{S_W^2}{C_W}S_\theta + 2X_{f_{Ra}}\frac{g_X}{g}, \quad (34)$$

where Q_f and X_f are the corresponding electric and $U(1)_X$ charges of the fermion f, while I_3 is the isospin which is 1 for the upper components and -1 for the lower ones. For future reference, we list explicitly in Tables II and III the neutral currents for each flavor fermion. We emphasize that particles such as $e_L^{e,\mu}$, $\nu_L^{e,\mu}$, $u_L^{2,3}$ and $d_L^{2,3}$ are devoid of couplings with g_X, which is a consequence of their zero $U(1)_X$ charge.

For the newly fermions, labeled with the index α, both the left-handed and right-handed are singlets of $SU(2)_L$. Thus, the neutral current couplings are:

$$g_{L,Rm}^{(f_a)} = T_W Y_{f_{L,R\alpha}}(R_0^T)_{2m} + \frac{2g_X}{g}X_{f_{L,R\alpha}}(R_0^T)_{3m}, \quad (35)$$

which are listed in Tables IV and V for each flavor of this sector.

On the other hand, according to (13), the fermion fields must be also rotated into a mass eigenstate basis. By labeling $\tilde{f}_i$ each component of the mass basis $\tilde{\mathbf{f}}$ and f_i the corresponding in weak basis, the transformation (13) are written in components as:

$$\tilde{f}_{L,Ri} = (V_{L,R}^{f\dagger})_{ij}f_{L,Rj}. \quad (36)$$

Thus, the neutral current Lagrangian (30) in full mass eigenstates is

$$\mathcal{L}_{NC} = \frac{g}{2}\Big[\overline{\tilde{f}_{Li}}\gamma_\mu\tilde{V}_m^\mu(V_L^{f\dagger})_{ij}g_{Lm}^{(f_j)}(V_L^f)_{jk}\tilde{f}_{Lk} + \overline{\tilde{f}_{Ri}}\gamma_\mu\tilde{V}_m^\mu(V_R^{f\dagger})_{ij}g_{Rm}^{(f_j)}(V_R^f)_{jk}\tilde{f}_{Rk}\Big]. \quad (37)$$

In mass eigenstates, the neutral current couplings transform through the fermionic biunitary matrices:

$$g_{L,Rm}^{(f_j)} \to \tilde{g}_{L,Rm}^{(ik)} = (V_{L,R}^{f\dagger})_{ij}g_{L,Rm}^{(f_j)}(V_{L,R}^f)_{jk}, \quad (38)$$

so, the neutral Lagrangian (37) become:

$$\mathcal{L}_{NC} = \frac{g}{2}\Big[\overline{\tilde{f}_{Li}}\gamma_\mu\tilde{V}_m^\mu\tilde{g}_{Lm}^{(jk)}\tilde{f}_{Lk} + \overline{\tilde{f}_{Ri}}\gamma_\mu\tilde{V}_m^\mu\tilde{g}_{Rm}^{(jk)}\tilde{f}_{Rk}\Big]. \quad (39)$$

In general, as shown in Tables II–V, there are couplings that are family dependent. For these cases, the neutral couplings $\tilde{g}_{L,R}^{(ik)}$ are nondiagonal, producing FCNC processes, such as in the dilepton B decay. For the family universal couplings, due to the unitary constraint in (15), the neutral couplings

TABLE II. Neutral current couplings for the ordinary SM left-handed fermions.

f_{La}	$g_{L1}^{(f_a)}$	$g_{L2}^{(f_a)}$	$g_{L3}^{(f_a)}$
u_L^1	$\frac{4}{3}S_W$	$(1-\frac{4}{3}S_W^2)\frac{1}{C_W}+\frac{2g_X}{3g}S_\theta$	$(-1+\frac{4}{3}S_W^2)\frac{S_\theta}{C_W}+\frac{2g_X}{3g}$
$u_L^{2,3}$	$\frac{4}{3}S_W$	$(1-\frac{4}{3}S_W^2)\frac{1}{C_W}$	$(-1+\frac{4}{3}S_W^2)\frac{S_\theta}{C_W}$
d_L^1	$-\frac{2}{3}S_W$	$(-1+\frac{2}{3}S_W^2)\frac{1}{C_W}+\frac{2g_X}{3g}S_\theta$	$(1-\frac{2}{3}S_W^2)\frac{S_\theta}{C_W}+\frac{2g_X}{3g}$
$d_L^{2,3}$	$-\frac{2}{3}S_W$	$(-1+\frac{2}{3}S_W^2)\frac{1}{C_W}$	$(1-\frac{2}{3}S_W^2)\frac{S_\theta}{C_W}$
$e_L^{e,\mu}$	$-2S_W$	$(-1+2S_W^2)\frac{1}{C_W}$	$(1-2S_W^2)\frac{S_\theta}{C_W}$
e_L^τ	$-2S_W$	$(-1+2S_W^2)\frac{1}{C_W}-\frac{2g_X}{g}S_\theta$	$(1-2S_W^2)\frac{S_\theta}{C_W}-\frac{2g_X}{g}$
$\nu_L^{e,\mu}$	0	$\frac{1}{C_W}$	$\frac{S_\theta}{C_W}$
ν_L^τ	0	$\frac{1}{C_W}-\frac{2g_X}{g}S_\theta$	$-\frac{S_\theta}{C_W}-\frac{2g_X}{g}$

TABLE III. Neutral current couplings for the ordinary SM right-handed fermions.

f_{Ra}	$g_{R1}^{(f_a)}$	$g_{R2}^{(f_a)}$	$g_{R3}^{(f_a)}$
$u_R^{1,2,3}$	$\frac{4}{3}S_W$	$-\frac{4}{3}(\frac{S_W^2}{C_W}-\frac{g_X}{g}S_\theta)$	$\frac{4}{3}(\frac{S_W^2}{C_W}S_\theta+\frac{g_X}{g})$
$d_R^{1,2,3}$	$-\frac{2}{3}S_W$	$\frac{2}{3}(\frac{S_W^2}{C_W}-\frac{g_X}{g}S_\theta)$	$-\frac{2}{3}(\frac{S_W^2}{C_W}S_\theta+\frac{g_X}{g})$
$e_R^{e,\tau}$	$-2S_W$	$\frac{8}{3}(\frac{3}{4}\frac{S_W^2}{C_W}-\frac{g_X}{g}S_\theta)$	$-\frac{8}{3}(\frac{3}{4}\frac{S_W^2}{C_W}S_\theta+\frac{g_X}{g})$
e_R^μ	$-2S_W$	$\frac{2}{3}(3\frac{S_W^2}{C_W}-\frac{g_X}{g}S_\theta)$	$-\frac{2}{3}(3\frac{S_W^2}{C_W}S_\theta+\frac{g_X}{g})$

TABLE IV. Neutral current couplings for the newly left-handed fermions.

$f_{L\alpha}$	$g_{L1}^{(f_a)}$	$g_{L2}^{(f_a)}$	$g_{L3}^{(f_a)}$
$\mathcal{T}_L$	$\frac{4}{3}S_W$	$-\frac{2}{3}(2\frac{S_W^2}{C_W}-\frac{g_X}{g}S_\theta)$	$\frac{2}{3}(2\frac{S_W^2}{C_W}S_\theta+\frac{g_X}{g})$
$\mathcal{J}_L^{1,2}$	$-\frac{2}{3}S_W$	$\frac{2}{3}\frac{S_W^2}{C_W}$	$-\frac{2}{3}\frac{S_W^2}{C_W}S_\theta$
$\mathcal{E}_L^1$	$-2S_W$	$2(\frac{S_W^2}{C_W}-\frac{g_X}{g}S_\theta)$	$-2(\frac{S_W^2}{C_W}S_\theta+\frac{g_X}{g})$
$\mathcal{E}_L^2$	$-2S_W$	$\frac{4}{3}(\frac{3}{2}\frac{S_W^2}{C_W}-\frac{g_X}{g}S_\theta)$	$-\frac{4}{3}(\frac{3}{2}\frac{S_W^2}{C_W}S_\theta+\frac{g_X}{g})$

TABLE V. Neutral current couplings for the newly right-handed fermions.

$f_{R\alpha}$	$g_{R1}^{(f_a)}$	$g_{R2}^{(f_a)}$	$g_{R3}^{(f_a)}$
$\mathcal{T}_R$	$\frac{4}{3}S_W$	$-\frac{4}{3}(\frac{S_W^2}{C_W}-\frac{g_X}{g}S_\theta)$	$\frac{4}{3}(\frac{S_W^2}{C_W}S_\theta+\frac{g_X}{g})$
$\mathcal{J}_R^{1,2}$	$-\frac{2}{3}S_W$	$\frac{2}{3}(\frac{S_W^2}{C_W}-\frac{g_X}{g}S_\theta)$	$-\frac{2}{3}(\frac{S_W^2}{C_W}S_\theta+\frac{g_X}{g})$
$\mathcal{E}_R^1$	$-2S_W$	$\frac{4}{3}(\frac{3}{2}\frac{S_W^2}{C_W}-\frac{g_X}{g}S_\theta)$	$-\frac{4}{3}(\frac{3}{2}\frac{S_W^2}{C_W}S_\theta+\frac{g_X}{g})$
$\mathcal{E}_R^2$	$-2S_W$	$2(\frac{S_W^2}{C_W}-\frac{g_X}{g}S_\theta)$	$-2(\frac{S_W^2}{C_W}S_\theta+\frac{g_X}{g})$
$\nu_R^{1,2,3}$	0	$\frac{2}{3}\frac{g_X}{g}S_\theta$	$\frac{2}{3}\frac{g_X}{g}$
$\mathcal{N}_R^{1,2,3}$	0	0	0

become diagonal, $\tilde{g}^{(ik)}_{L,R} = g^{(f_j)}_{L,R}\delta_{ik}$, which only produce flavor conservative neutral currents.

III. B DECAY

The process $B^+ \to K^+\ell^+\ell^-$ for charged leptons $\ell^\pm$ is due to $b \to s\ell^+\ell^-$ transitions. In the model, this process can be induced at tree level through the neutral weak bosons Z_1 and Z_2 as shown in Fig. 1.

A. Fundamental couplings

1. The $b-s-Z_{1(2)}$ coupling

First, according to the neutral current Lagrangian in (39), the FCNC transition $b \to s$ in the first vertex of Fig. 1, is described by the Lagrangian:

$$\mathcal{L}_{sb} = \frac{g}{2}[\overline{s_L}\gamma_\mu(Z_1^\mu \tilde{g}^{(23)}_{L2} + Z_2^\mu \tilde{g}^{(23)}_{L3})b_L + \overline{s_R}\gamma_\mu(Z_1^\mu \tilde{g}^{(23)}_{R2} + Z_2^\mu \tilde{g}^{(23)}_{R3})b_R] + \text{H.c.}, \quad (40)$$

where:

$$\tilde{g}^{(23)}_{L,Rm} = (V^{D\dagger}_{L,R})_{2j} g^{(D_j)}_{L,Rm} (V^D_{L,R})_{j3}, \quad (41)$$

with $D_j = (d_1, d_2, d_3, \mathcal{J}_1, \mathcal{J}_2)$. Separating the ordinary fermions $D_a = (d_1, d_2, d_3)$ from the new ones $D_\alpha = (\mathcal{J}_1, \mathcal{J}_2)$, we can write the above coupling as:

$$\tilde{g}^{(23)}_{L,Rm} = (V^{D\dagger}_{L,R})_{2a} g^{(D_a)}_{L,Rm} (V^D_{L,R})_{a3} + (V^{D\dagger}_{L,R})_{2\alpha} g^{(D_\alpha)}_{L,Rm} (V^D_{L,R})_{\alpha 3}. \quad (42)$$

Taking into account that according to Tables II–V for the down-type sector, only the left-handed ordinary down quarks exhibits family dependence, then the left-handed couplings in (42) expands as:

$$\tilde{g}^{(23)}_{Lm} = g^{(d_1)}_{Lm}(V^{D\dagger}_L)_{21}(V^D_{L,R})_{13} + g^{(d_{2,3})}_{Lm}[(V^{D\dagger}_L)_{22}(V^D_{L,R})_{23} + (V^{D\dagger}_{L,R})_{23}(V^D_{L,R})_{33}] + g^{(D_\alpha)}_{Lm}(V^{D\dagger}_L)_{2\alpha}(V^D_{L,R})_{\alpha 3}, \quad (43)$$

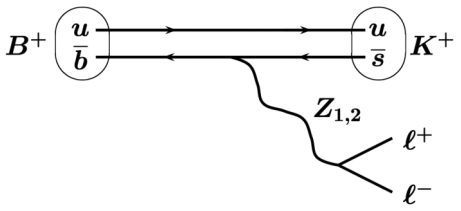

FIG. 1. Decay $B^+ \to K^+\ell^+\ell^-$ through neutral gauge bosons $Z_{1,2}$.

while the right-handed couplings (family universal) cancel out,

$$\tilde{g}^{(23)}_{Rm} = 0. \quad (44)$$

From the unitary constraint (18), we find the following relation:

$$(V^{D\dagger}_L)_{22}(V^D_L)_{23} + (V^{D\dagger}_L)_{23}(V^D_L)_{33} = -(V^{D\dagger}_L)_{21}(V^D_L)_{13} - (V^{D\dagger}_L)_{2\alpha}(V^D_L)_{\alpha 3}, \quad (45)$$

which, after replacing in (43), we obtain:

$$\tilde{g}^{(23)}_{Lm} = (V^{D\dagger}_L)_{21}(V^D_L)_{13}[g^{(d_1)}_{Lm} - g^{(d_{2,3})}_{Lm}] + (V^{D\dagger}_L)_{2\alpha}(V^D_L)_{\alpha 3}[g^{(D_\alpha)}_{Lm} - g^{(d_{2,3})}_{Lm}]. \quad (46)$$

We see that in a family universal scenario, where the coupling $g^{(d_{2,3})}_{Lm}$ would be the same as for $g^{(d_1)}_{Lm}$ and $g^{(D_\alpha)}_{Lm}$, the above coupling cancel out, suppressing the FCNC transition $b \to s$. However, the model distinguish these couplings, according to the family index. Specifically, using the values from Table II, we obtain the left-handed neutral couplings for the $b-s$ interaction shown in the first row from Table VI.

2. The $e^+(\mu^+)-e^-(\mu^-)-Z_{1(2)}$ coupling

On the other hand, the neutral coupling for the decays $Z_{1,2} \to \ell^+_a\ell^-_a$ in the second vertex from Fig. 1 for $\ell_a = e$ and μ, is described by:

$$\mathcal{L}_\ell = \frac{g}{2}\left[\overline{\ell_{La}}\gamma_\mu(Z_1^\mu \tilde{g}^{(aa)}_{L2} + Z_2^\mu \tilde{g}^{(aa)}_{L3})\ell_{La} + \overline{\ell_{Ra}}\gamma_\mu(Z_1^\mu \tilde{g}^{(aa)}_{R2} + Z_2^\mu \tilde{g}^{(aa)}_{R3})\ell_{Ra}\right], \quad (47)$$

with

$$\tilde{g}^{(aa)}_{L,Rm} = (V^{E\dagger}_{L,R})_{aj} g^{(E_j)}_{L,Rm} (V^E_{L,R})_{ja}, \quad (48)$$

for $E_j = (e^e, e^\mu, e^\tau, \mathcal{E}_1, \mathcal{E}_2)$. By using the unitary constraint, we obtain for the left-handed couplings of the charged leptons:

$$\tilde{g}^{(aa)}_{Lm} = g^{(e^e,e^\mu)}_{Lm} + |(V^E_L)_{3a}|^2[g^{(e^\tau)}_{Lm} - g^{(e^e,e^\mu)}_{Lm}] + |(V^E_L)_{\alpha a}|^2[g^{(E_\alpha)}_{Lm} - g^{(e^e,e^\mu)}_{Lm}], \quad (49)$$

and for the right-handed ones, we obtain:

$$\tilde{g}^{(aa)}_{Rm} = g^{(e^e,e^\tau)}_{Rm} + |(V^E_R)_{2a}|^2[g^{(e^\mu)}_{Rm} - g^{(e^e,e^\tau)}_{Rm}] + |(V^E_R)_{\alpha a}|^2[g^{(E_\alpha)}_{Rm} - g^{(e^e,e^\tau)}_{Rm}]. \quad (50)$$

In this case, we see that the first term of the above equations do not depend on the flavor number a (it is the same for $e^{\pm}$ as for $\mu^{\pm}$). However, the subsequent terms depends explicitly from the ia components of the fermionic biunitary matrices, due to the nonuniversality of the neutral couplings. Since, in general, each component of the matrices are different, we will obtain a distinction between the couplings to electrons and to muons. As a consequence, the ratio of the branching of the $B^+ \to K^+ e^+ e^-$ and $B^+ \to K^+ \mu^+ \mu^-$ deviates from one, as suggests the LHCb data. Again, using the values from Tables II–V for the charged leptons, we obtain the neutral couplings for $Z_{1,2} \to e^{\pm}(\mu^{\pm})$ in Tables VI and VII, for left- and right-handed leptons, respectively.

B. Effective operators

From the neutral Lagrangians in (40) and (47), we obtain the matrix element for the $b \to s\ell_a^+\ell_a^-$ process:

$$i\mathcal{M}_{fi} = -\frac{ig^2}{4}[\overline{u_s}\gamma_\mu(\tilde{g}_{Lm}^{(23)}L)u_b]D^{\mu\nu}[\overline{u_a}\gamma_\nu(\tilde{g}_{Lm}^{(aa)}L + \tilde{g}_{Rm}^{(aa)}R)v_a], \tag{51}$$

where $u_{s,b,a}$ are the wave functions of the fermions s, b, and ℓ_a, respectively, and v_a of antileptons $\bar{\ell}_a$, while $D^{\mu\nu}$ is the propagator of the intermediary gauge bosons, defined in the Feynman gauge as:

$$D^{\mu\nu} = \frac{-ig^{\mu\nu}}{q^2 - M_{Z_m}^2}. \tag{52}$$

At low energies, the momentum transfer through the intermediary particles is negligible in relation to their masses. Thus, the above matrix element become:

$$i\mathcal{M}_{fi} \approx -\frac{ig^2}{4M_{Z_m}^2}\overline{u_s}\gamma_\mu(\tilde{g}_{Lm}^{(23)}L)u_b\overline{u_a}\gamma^\mu(\tilde{g}_{Lm}^{(aa)}L + \tilde{g}_{Rm}^{(aa)}R)v_a. \tag{53}$$

The above matrix element can be derived from the following effective Hamiltonian:

$$\mathcal{H}_{\text{eff}}^{\text{NP}} = \frac{g^2}{4M_{Z_m}^2}[\bar{s}(\tilde{g}_{Lm}^{(23)}\gamma_\mu L)b]\left[\overline{\ell_a}\gamma^\mu(\tilde{g}_{Lm}^{(aa)}L + \tilde{g}_{Rm}^{(aa)}R)\ell_a\right] + \text{H.c.}, \tag{54}$$

where NP is the label for new non-SM physics, which affect the ordinary SM contribution, described by the Wilson operators through the effective Hamiltonian [18–20]:

$$\mathcal{H}_{\text{eff}}^{\text{SM}} = -\frac{4G_F}{\sqrt{2}}V_{tb}V_{ts}^*\sum_i[C_i^{\text{SM}}\mathcal{O}_i + C_i'^{\text{SM}}\mathcal{O}_i'] + \text{H.c.}, \tag{55}$$

where the dominant Wilson coefficients are $C_i^{\text{SM}} = C_{9,10}^{\text{SM}}$, with

$$\mathcal{O}_9 = \frac{\alpha_{\text{em}}}{4\pi}[\bar{s}\gamma_\mu Lb][\overline{\ell_a}\gamma^\mu\ell_a],$$
$$\mathcal{O}_{10} = \frac{\alpha_{\text{em}}}{4\pi}[\bar{s}\gamma_\mu Lb][\overline{\ell_a}\gamma^\mu\gamma_5\ell_a]. \tag{56}$$

TABLE VI. Neutral current couplings for the left-handed fermions $b - s$, $e^{\pm}$, and $\mu^{\pm}$.

$\bar{f}_a f_b$	$\tilde{g}_{L2}^{(ab)}$	$\tilde{g}_{L3}^{(ab)}$
$\bar{s}b$	$\frac{2}{3}\frac{g_X}{g}(V_L^{D\dagger})_{21}(V_L^D)_{13}S_\theta + \frac{1}{C_W}(V_L^{D\dagger})_{2\alpha}(V_L^D)_{\alpha 3}$	$\frac{2}{3}\frac{g_X}{g}(V_L^{D\dagger})_{21}(V_L^D)_{13} - \frac{1}{C_W}(V_L^{D\dagger})_{2\alpha}(V_L^D)_{\alpha 3}S_\theta$
e^+e^-	$(-1+2S_W^2)\frac{1}{C_W} - 2\frac{g_X}{g}\lvert(V_L^E)_{31}\rvert^2 S_\theta$	$(1-2S_W^2)\frac{S_\theta}{C_W} - 2\frac{g_X}{g}\lvert(V_L^E)_{31}\rvert^2$
	$+(\frac{1}{C_W} - 2\frac{g_X}{g}S_\theta)\lvert(V_L^E)_{41}\rvert^2 + (\frac{1}{C_W} - \frac{4}{3}\frac{g_X}{g}S_\theta)\lvert(V_L^E)_{51}\rvert^2$	$-(\frac{S_\theta}{C_W} + 2\frac{g_X}{g})\lvert(V_L^E)_{41}\rvert^2 - (\frac{S_\theta}{C_W} + \frac{4}{3}\frac{g_X}{g})\lvert(V_L^E)_{51}\rvert^2$
$\mu^+\mu^-$	$(-1+2S_W^2)\frac{1}{C_W} - 2\frac{g_X}{g}\lvert(V_L^E)_{32}\rvert^2 S_\theta$	$(1-2S_W^2)\frac{S_\theta}{C_W} - 2\frac{g_X}{g}\lvert(V_L^E)_{32}\rvert^2$
	$+(\frac{1}{C_W} - 2\frac{g_X}{g}S_\theta)\lvert(V_L^E)_{42}\rvert^2 + (\frac{1}{C_W} - \frac{4}{3}\frac{g_X}{g}S_\theta)\lvert(V_L^E)_{52}\rvert^2$	$-(\frac{S_\theta}{C_W} + 2\frac{g_X}{g})\lvert(V_L^E)_{42}\rvert^2 - (\frac{S_\theta}{C_W} + \frac{4}{3}\frac{g_X}{g})\lvert(V_L^E)_{52}\rvert^2$

TABLE VII. Neutral current couplings for the right-handed fermions $b - s$, $e^{\pm}$, and $\mu^{\pm}$.

$\bar{f}_a f_b$	$\tilde{g}_{R2}^{(ab)}$	$\tilde{g}_{R3}^{(ab)}$
$\bar{s}b$	0	0
e^+e^-	$\frac{8}{3}(\frac{3}{4}\frac{S_W^2}{C_W} - \frac{g_X}{g}S_\theta) + 2\frac{g_X}{g}\lvert(V_R^E)_{21}\rvert^2 S_\theta$	$-\frac{8}{3}(\frac{3}{4}\frac{S_W^2}{C_W}S_\theta + \frac{g_X}{g}) + 2\frac{g_X}{g}\lvert(V_R^E)_{21}\rvert^2$
	$+\frac{4}{3}\frac{g_X}{g}\lvert(V_R^E)_{41}\rvert^2 S_\theta + \frac{2}{3}\frac{g_X}{g}\lvert(V_R^E)_{51}\rvert^2 S_\theta$	$\frac{4}{3}\frac{g_X}{g}\lvert(V_R^E)_{41}\rvert^2 + \frac{2}{3}\frac{g_X}{g}\lvert(V_R^E)_{51}\rvert^2$
$\mu^+\mu^-$	$\frac{8}{3}(\frac{3}{4}\frac{S_W^2}{C_W} - \frac{g_X}{g}S_\theta) + 2\frac{g_X}{g}\lvert(V_R^E)_{22}\rvert^2 S_\theta$	$-\frac{8}{3}(\frac{3}{4}\frac{S_W^2}{C_W}S_\theta + \frac{g_X}{g}) + 2\frac{g_X}{g}\lvert(V_R^E)_{22}\rvert^2$
	$+\frac{4}{3}\frac{g_X}{g}\lvert(V_R^E)_{42}\rvert^2 S_\theta + \frac{2}{3}\frac{g_X}{g}\lvert(V_R^E)_{52}\rvert^2 S_\theta$	$\frac{4}{3}\frac{g_X}{g}\lvert(V_R^E)_{42}\rvert^2 + \frac{2}{3}\frac{g_X}{g}\lvert(V_R^E)_{52}\rvert^2$

Putting together both Hamiltonians, Eqs. (54) and (55), and taking the approximated value of

$$\frac{G_F \alpha_{\rm em}}{\sqrt{2}\pi} V_{tb} V_{ts}^* \approx \frac{1}{(36\ \text{TeV})^2}, \tag{57}$$

we obtain the total effective Hamiltonian:

$$\begin{aligned}\mathcal{H}_{\rm eff} &= \mathcal{H}_{\rm eff}^{\rm SM} + \mathcal{H}_{\rm eff}^{\rm NP} \\ &= -\frac{1}{(36\,\text{TeV})^2}\left[C_9^{\rm SM} - \frac{g^2(36\,\text{TeV})^2}{8M_{Z_m}^2}\tilde{g}_{Lm}^{(23)}(\tilde{g}_{Lm}^{(aa)} + \tilde{g}_{Rm}^{(aa)})\right] \\ &\times (\bar{s}\gamma_\mu L b)(\overline{\ell_a}\gamma^\mu \ell_a) \\ &-\frac{1}{(36\,\text{TeV})^2}\left[C_{10}^{\rm SM} + \frac{g^2(36\,\text{TeV})^2}{8M_{Z_m}^2}\tilde{g}_{Lm}^{(23)}(\tilde{g}_{Lm}^{(aa)} - \tilde{g}_{Rm}^{(aa)})\right] \\ &\times (\bar{s}\gamma_\mu L b)(\overline{\ell_a}\gamma^\mu\gamma_5 \ell_a),\end{aligned} \tag{58}$$

from where we identify the total Wilson coefficients:

$$C_9^{(a)} = C_9^{\rm SM} + C_9^{NP(a)}, \qquad C_{10}^{(a)} = C_{10}^{\rm SM} + C_{10}^{NP(a)}, \tag{59}$$

with:

$$C_9^{NP(a)} = -\frac{g^2(36\ \text{TeV})^2}{8M_{Z_m}^2}\tilde{g}_{Lm}^{(23)}(\tilde{g}_{Lm}^{(aa)} + \tilde{g}_{Rm}^{(aa)}) \tag{60}$$

$$C_{10}^{NP(a)} = \frac{g^2(36\ \text{TeV})^2}{8M_{Z_m}^2}\tilde{g}_{Lm}^{(23)}(\tilde{g}_{Lm}^{(aa)} - \tilde{g}_{Rm}^{(aa)}), \tag{61}$$

where a sum over repeated indices $m = \{1, 2\}$ is implied in the right terms. For the SM contributions, we use the values $C_9^{\rm SM} \approx -C_{10}^{\rm SM} \approx 4.1$ [20].

C. $e-\mu$ relative branching ratio

The LHCb collaboration recorded a measurement of the ratio of the branching fractions of $B^+ \to K^+\mu^+\mu^-$ and $B^+ \to K^+e^+e^-$ decay, which is given by:

$$R_K = \frac{\int_{q^2_{\rm min}}^{q^2_{\rm max}} \frac{d\Gamma[B^+\to K^+\mu^+\mu^-]}{dq^2} dq^2}{\int_{q^2_{\rm min}}^{q^2_{\rm max}} \frac{d\Gamma[B^+\to K^+e^+e^-]}{dq^2} dq^2}, \tag{62}$$

within the dilepton invariant mass squared range $1 < q^2 < 6\ \text{GeV}^2/c^4$. In terms of the Wilson coefficients, R_K is [21]:

$$R_K = \frac{|C_9^{(\mu)}|^2 + |C_{10}^{(\mu)}|^2}{|C_9^{(e)}|^2 + |C_{10}^{(e)}|^2}. \tag{63}$$

By expanding the coefficients in SM and NP contributions according to (59), and taking into accout the lepton universality of the SM, we obtain:

$$R_K = \frac{|C_9^{\rm SM} + C_9^{NP(\mu)}|^2 + |C_{10}^{\rm SM} + C_{10}^{NP(\mu)}|^2}{|C_9^{\rm SM} + C_9^{NP(e)}|^2 + |C_{10}^{\rm SM} + C_{10}^{NP(e)}|^2}. \tag{64}$$

By assuming that the above expression corresponds to the experimentally measured, we can fit the free parameters of the model according to the reported value [7]

$$R_K = 0.745^{+0.090}_{-0.074} \pm 0.036. \tag{65}$$

The free parameters are classified into two categories. First, the gauge parameters, corresponding to the Z' gauge boson mass, the gauge coupling constant of the $U(1)_X$ symmetry, and the $Z - Z'$ mixing angle: $(M_{Z'}, g_X, S_\theta)$. Second, the fermion parameters which arise from the biunitary transformations that rotate the fermion flavors into mass states, according to (13), and that depend from the Yukawa couplings and the VEVs of the Higgs fields. By using the scheme shown in Ref. [14], these matrices can be parametrized as functions of mixing angles. After some simplifications, as shown in Appendix B, we are left with six free parameters: two ratios of Yukawa couplings, $r_{\mathcal{J}} = h_{\mathcal{J}}/h_u$ and $r_{\mathcal{E}} = h_{\mathcal{E}}/h_u$, where $h_{\mathcal{J},\mathcal{E}}$ are the couplings of the extra charged fermions shown in the matrices in Eqs. (B22) and (B26), while h_u is the coupling of the ordinary up-type quarks according to (B20), the two masses m_J and m_E, corresponding to the new down-type quarks and charged leptons, and two mixing angles from the left- and right-handed charged leptons, $\theta_{13}^{E_L}$ and $\theta_{25}^{E_R}$, which we express through their tangents $t_{13}^{E_L}$ and $t_{25}^{E_R}$. All other mixing angles can be written as function of these two angles, as shown in Eq. (B28). In particular, as shown in Tables VI and VII, the neutral current couplings depends on the $ij = 2a$, $3a$, $4a$, and $5a$ bi-unitary components with $a = 1$ for electrons and 2 for muons. Explicitly these components can be fully written as functions of $\theta_{13}^{E_L}$ and $\theta_{25}^{E_R}$, as shown in Eqs. (B30) and (B31).

Thus, the space of parameters is reduced to 9 variables: $(M_{Z'}, m_J, m_E, g_X, r_{\mathcal{J}}, r_{\mathcal{E}}, S_\theta, t_{13}^{E_L}, t_{25}^{E_R})$. However, some of these parameters are constrained from theoretical conditions and other experimental observables. For example, the mass $M_{Z'}$ has lower limits from direct detection in colliders. Experiments at LHC collected data at $\sqrt{s} = 13$ TeV for new resonances in dielectron and dimuon final states, where lower limits on $M_{Z'}$ between 3.5 TeV and 4.5 TeV at 36.1 fb^{-1} by the ATLAS collaboration, and 3.5 TeV and 4 TeV at 12.4 fb^{-1} by CMS are reported [22]. We take the lowest experimental limit of 3.5 TeV. Also, in models with extra gauge neutral bosons, the $Z - Z'$ mixing angle is suppressed as the inverse of the squared Z'-mass and by electroweak observables, to values up to $\sim 10^{-3}$, which has a negligible effect on the total branching decays. Thus, for simplicity, we ignore this mixing and take $S_\theta = 0$. The coupling g_X is constrained by Z' production limits. For example, in some models with the same gauge couplings as

the model proposed here, limits on dilepton events $pp \to Z' \to \ell\ell$ at LHC allow values as large as $g_X \approx 0.4$ [12,16]. Search for extra fermions can change according to specific model-dependent assumptions [23]. We use a safe scenery with mass values around the TeV scale. Finally, we assume one common Yukawa ratio $r_h = r_{\mathcal{J}} = r_{\mathcal{E}}$.

In summary, if we fix the parameters as described above, we are left with three free parameters, two mixing angles and one Yukawa ratio $(t_{13}^{E_L}, t_{25}^{E_R}, r_h)$, which we fit according to the experimental bound in (65). The first aspect to note is that the couplings to electrons have contributions from the biunitary components $(V_L^E)_{a1}$ for $a = 3, 4, 5$ and $(V_R^E)_{a1}$ for $a = 2, 4, 5$, while the muons couple through $(V_L^E)_{a2}$ and $(V_R^E)_{a2}$, as can be verified in tables VI and VII. So, the flavor nonuniversality in the model arise from the difference between the $a1$ and $a2$ components of the biunitary matrices, which occur according to Eqs. (B30) and (B31). The plots in Fig. 2 highlight the difference between electrons and muons components as function of the mixing tangent $t_{13}^{E_L}$, where we have fixed the other parameters in an arbitrary form, which only will shift the curves but does not change their fundamental form. We see that for the left-handed leptons in the first plot, the 31 (red continuous curve) and 32 (blue continuous curve) components exhibit a small difference, which favored a universal lepton coupling. The largest lepton universality violation occur due to the 41 and 42 components near to $t_{13}^{E_L} = 0.13$. The right-handed leptons, on the other hand, exhibit larger violation terms than the left-handed ones, due mainly to the 21 and 22 components, as shown in the second plot. The largest differences occur for $t_{13}^{E_L}$ far from 1, which may generate two scenarios: for small and for large $t_{13}^{E_L}$ mixing. However, as we will discuss below, this angle is suppressed as the muon to top quark mass ratio m_μ/m_t, thus the scenery with small $t_{13}^{E_L}$ will be favored.

Numerically, we found that the reported anomaly can be fitted only for large Yukawa ratios, above $r_h \gtrsim 45$, i.e., the Yukawa couplings that mix the new fermions $\mathcal{J}$ and $\mathcal{E}$ with the ordinary SM fermions must be larger than the couplings among the ordinary up-type quarks in a factor of the order of 4.5×10^1, which corresponds to the order of the absolute values if we assume couplings of the ordinary particles at the order of 1. An important implication to have large Yukawa couplings is the possibility to find a Landau pole in the Yukawa coupling below the Planck scale, which would reduce the perturbative regimen of the model. A deep analysis in this aspect require a careful study of the renormalization group equations of the theory, which falls outside the scope of this work.

Regarding the mixing angles, the left plot in Fig. 3 displays allowed points in the $(t_{13}^{E_L}, t_{25}^{E_R})$ plane for $r_h = 50$, where a small but non-null mixing angle $\theta_{13}^{E_L}$ is require, while $\theta_{25}^{E_R}$ can be as large as 42°, which occur for $\theta_{13}^{E_L} \approx 4.6°$. According to (B18), a $\theta_{25}^{E_R}$ mixing angle near 45° (i.e., $t_{25}^{E_R} \sim 1$) represents an scenery where all the couplings with the new leptons $\mathcal{E}$ have the same strength. However, most of the allowed points spread around a small 25 mixing, where the couplings of the new leptons is larger than their mixing coupling with the ordinary leptons. On the other hand, small $\theta_{13}^{E_L}$ mixing is expected according to (B14), where the tangent of this angle is proportional to the VEV ratio v_3/v_1. Since v_1 is proportional to the top quark mass, while v_3 is proportional to the muon mass as seen in Eqs. (B21) and (B27), then this mixing angle is suppressed by the ratio m_μ/m_t. If we increase the Yukawa ratio r_h, larger mixing angles can be obtained. The plot in the right of Fig. 3 shows contour plots for different ratios r_h from 50 to 90. Regarding the other mixing angles, they can be obtained from Eqs. (B28) and (B29) once $\theta_{13}^{E_L}$ and $\theta_{25}^{E_R}$ are fixed in accordance with the above allowed regions.

On the other hand, the branching ratio is also very sensitive to the masses of the extra fermions, m_E and m_J. To explore this, in Fig. 4 we display the allowed contours for the heavy quarks and charged leptons compatible with the limits in Fig. 3 for $r_h = 50$. We choose the two limits for the $\theta_{25}^{E_R}$ angle, at 0 and 0.8, for the central value $\theta_{13}^{E_L} = 0.08$. We see that large mass values of one fermion,

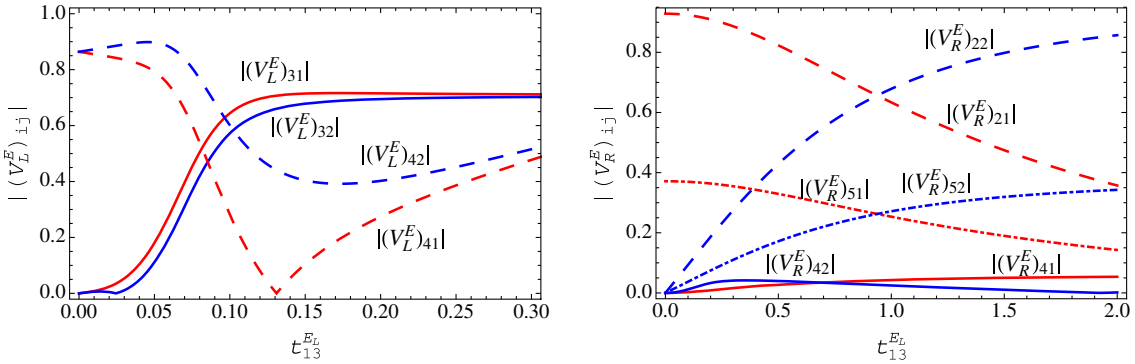

FIG. 2. Left-handed (V_L^E) and right-handed (V_R^E) biunitary components as function of the mixing tangent $t_{13}^{E_L}$ obtained from Eqs. (B30) and (B31). Each component ij couple to electrons when $j = 1$ (red lines) and to muons when $j = 2$ (blue lines).

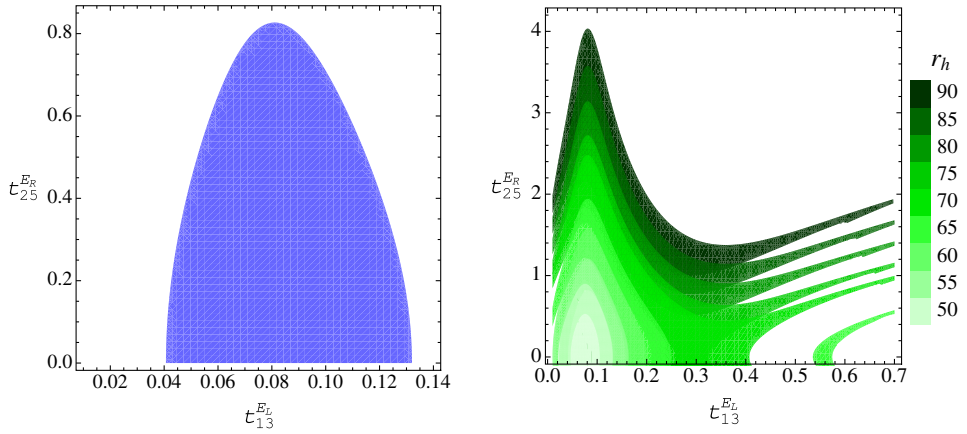

FIG. 3. Allowed points for the tangent of the mixing angles $\theta_{13}^{E_L}$ and $\theta_{25}^{E_R}$ for Yukawa ratio $r_h = 50$ (left plot), and for Yukawa ratios spanned from $r_h = 50$ to 90 (right plot) compatible with the experimental limit on R_K.

require smaller masses of the other one, which is confined in an energy range attainable by the LHC. Thus, the anomaly in the meson decay is compatible with new physics at the TeV scale.

In the above discussion, we assume real mixing rotations for the mass eigenstate transformations of the fermions. As a results, all the neutral current couplings in Tables VI and VII take real values. Now we want to explore the role of possible complex phases in the biunitary transformations. For the lepton couplings, we see in Tables VI and VII that the mixing matrices contributes as the squared of their magnitudes $|(V_L^E)_{ij}|$, so any complex phase associated to this sector does not have any effect in the branching ratios. For the quark couplings $\tilde{g}_{Lm}^{(23)}$, we see that they can be complex in general. In particular, if we neglect the $Z - Z'$ mixing angle, the only contribution to the $b \to s$ transition is the first term of $\tilde{g}_{L3}^{(23)}$, which may provide a relative complex phase between $(V_L^D)_{21}$ and $(V_L^D)_{13}$, which we call ϕ. Thus, in this more general scenario, the new physics of the Wilson coefficients in (60) and (61) will have a global complex term $e^{i\phi}$ coming from the coupling $\tilde{g}_{L3}^{(23)}$. If $\phi = 0$, we reproduce the same physics as shown above. If $\phi = \pi$, we obtain again real coefficients, but with opposite relative signs. For $0 < \phi < \pi$, the Wilson coefficients will have new complex contributions. In particular, if we take the same parameters as in Fig. 3, we can evaluate the ratio R_K for different values of the complex phase. For example, Fig. 5 shows the branching ratio as a function of the phase for $r_h = 50$, $t_{25}^{E_R} = 0$, and $t_{13}^{E_L}$ between the limits 0.04 and 0.12. The shaded band is the allowed region according to the reported anomaly. We first see that there are allowed solutions for small complex phases, obtaining the largest value at $\phi = \pi/4$ when $t_{13}^{E_L} = 0.08$. Second, we note that for $\phi = \pi$, the curves lies outside the allowed region. Thus, the sign (or more general, the phase) of the new physics

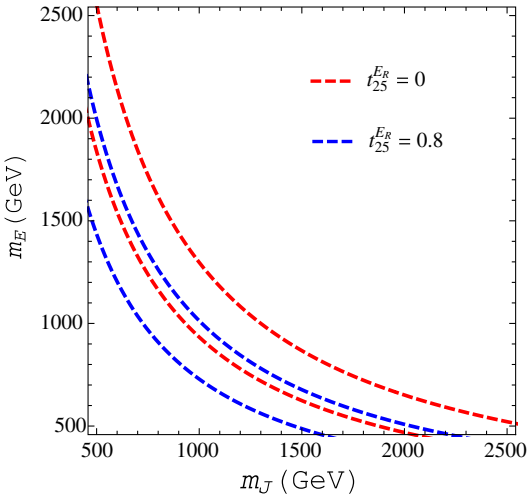

FIG. 4. Closed contours in the (m_J, m_E) plane for the extra fermion masses with central value $t_{13}^{E_L} = 0.08$ and the two limits $t_{25}^{E_R} = 0$ and 0.8, compatible with the allowed region from Fig. 3.

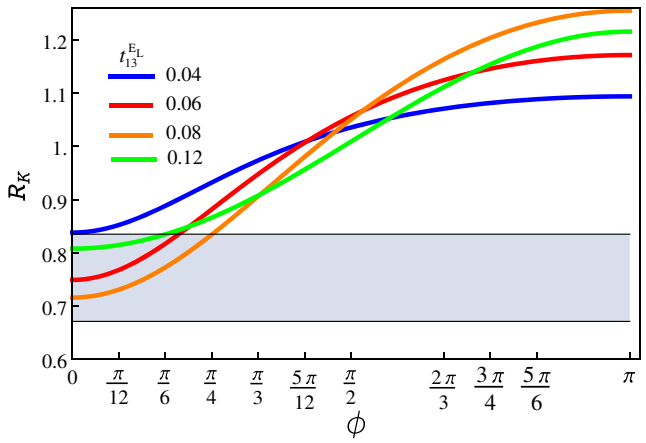

FIG. 5. Muon to electron branching ratio as function of the complex phase of $\tilde{g}_{L3}^{(23)}$ for $t_{25}^{E_R} = 0$ and $t_{13}^{E_L} = 0.04$, 0.06, 0.08, and 0.12. The shaded area is the reported bound.

contribution is essential to determine the best scenario to explain the observed anomaly.

IV. MODEL IN THE DECOUPLING LIMIT

The mixing couplings with the extra particles matter $\mathcal{E}^{1,2}$, $\mathcal{J}^{1,2}$, and $\mathcal{T}$ occurs through the fermionic biunitary matrices $(V_{L,R})_{i\alpha}$, with i the flavor index for the ordinary matter and α for the new matter. In the above section, we highlighted the importance of the new fermions in the simple scenary with "natural" parametrization. As a result, relatively large mixing couplings (strong coupling limit) is required in order to fit the observed anomaly of the B_s decay. If we reduce the mixing couplings to zero, i.e., if the $i\alpha$ components of the mass matrices are ignored, then we obtain the decoupling limit, where only ordinary fermions participate in the decay process. In particular, according to (B12) and (B14), the leptonic 13 left-handed mixing tangent would diverge ($t_{13}^{E_L} \to \infty$) in this limit, while from (B18) its 25 right-handed tangent would cancel out ($t_{25}^{E_R} = 0$). Figure 6 displays the branching ratio for different $t_{13}^{E_L}$ values and $t_{25}^{E_R} = 0$ as function of the Yukawa ratio r_h. We observe that for small $t_{13}^{E_L}$ values (below 1), there are solutions in the shaded region of the reported interval for R_K. However, for $t_{13}^{E_L} \geq 1$, the theoretical values of R_K increases above the allowed region. In the decoupling limit, with large θ_{13} angles, the branching ratio goes to the SM limit $R_K^{\mathrm{SM}} = 1$. Thus, the model in this scenario does not account for the reported anomaly. However, we can relax the natural parametrization to more general cases in order to obtain a feasible scenario in the decoupling limit. For that, we first reparametrize the neutral current couplings from Tables VI and VII in the decoupling limit as:

$$\begin{aligned}
\tilde{g}_{L2}^{(23)} &= \frac{2g_X}{3g}(V_L^{D\dagger})_{21}(V_L^D)_{13}S_\theta,\\
\tilde{g}_{L3}^{(23)} &= \frac{1}{S_\theta}\tilde{g}_{L2}^{(23)},\\
\tilde{g}_{L2}^{(aa)} &= -u_9 - \frac{2g_X}{g}|(V_L^E)_{3a}|^2 S_\theta,\\
\tilde{g}_{L3}^{(aa)} &= u_9 S_\theta - \frac{2g_X}{g}|(V_L^E)_{3a}|^2,\\
\tilde{g}_{R2}^{(aa)} &= u_{10} - u_9 + \frac{2g_X}{g}\left(-\frac{4}{3} + |(V_R^E)_{2a}|^2\right)S_\theta,\\
\tilde{g}_{R3}^{(aa)} &= (u_9 - u_{10})S_\theta + \frac{2g_X}{g}\left(-\frac{4}{3} + |(V_R^E)_{2a}|^2\right),
\end{aligned} \tag{66}$$

with

$$u_9 = \frac{1 - 2S_W^2}{C_W}, \qquad u_{10} = \frac{1}{C_W}. \tag{67}$$

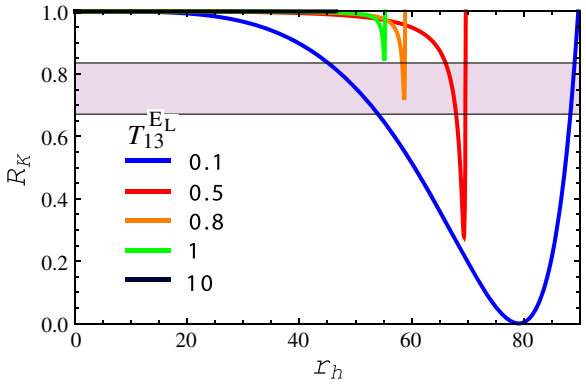

FIG. 6. Muon to electron branching ratio as function of the Yukawa coupling ratio r_h for $t_{25}^{E_R} = 0$ and $t_{13}^{E_L} = 0.1$, 0.5, 0.8, 1 and 10. The shaded area is the ratio experimentally reported in [7].

By ignoring the $Z - Z'$ mixing angle, the Wilson coefficients for new physics defined by (61) become:

$$\begin{aligned}
C_9^{NP(a)} &= \frac{g_X^2(36\ \mathrm{TeV})^2}{8M_{Z'}^2}K_9^{(a)},\\
C_{10}^{NP(a)} &= \frac{g_X^2(36\ \mathrm{TeV})^2}{8M_{Z'}^2}K_{10}^{(a)},
\end{aligned} \tag{68}$$

where the dependency on the flavor is separated in the coefficients

$$\begin{aligned}
K_9^{(a)} &= \frac{4}{3}(V_L^{D\dagger})_{21}(V_L^D)_{13}\left[\frac{4}{3} - |(V_R^E)_{2a}|^2 + |(V_L^E)_{3a}|^2\right],\\
K_{10}^{(a)} &= \frac{4}{3}(V_L^{D\dagger})_{21}(V_L^D)_{13}\left[\frac{4}{3} - |(V_R^E)_{2a}|^2 - |(V_L^E)_{3a}|^2\right].
\end{aligned} \tag{69}$$

Thus, the theoretical muon to electron branching ratio in (64) become:

$$R_K = \frac{\left|C_9^{\mathrm{SM}} + \frac{g_X^2(36\ \mathrm{TeV})^2}{8M_{Z'}^2}K_9^{(\mu)}\right|^2 + \left|C_{10}^{\mathrm{SM}} + \frac{g_X^2(36\ \mathrm{TeV})^2}{8M_{Z'}^2}K_{10}^{(\mu)}\right|^2}{\left|C_9^{\mathrm{SM}} + \frac{g_X^2(36\ \mathrm{TeV})^2}{8M_{Z'}^2}K_9^{(e)}\right|^2 + \left|C_{10}^{\mathrm{SM}} + \frac{g_X^2(36\ \mathrm{TeV})^2}{8M_{Z'}^2}K_{10}^{(e)}\right|^2}. \tag{70}$$

In order to compare with the experimental data, we define the new physics deviation as:

$$\begin{aligned}
\Delta C_a = &\sqrt{\left|C_9^{\mathrm{SM}} + C_9^{NP(a)}\right|^2 + \left|C_{10}^{\mathrm{SM}} + C_{10}^{NP(a)}\right|^2}\\
&- \sqrt{|C_9^{\mathrm{SM}}|^2 + |C_{10}^{\mathrm{SM}}|^2},
\end{aligned} \tag{71}$$

so, the ratio (70) become:

$$R_K = \left(\frac{\sqrt{|C_9^{\rm SM}|^2 + |C_{10}^{\rm SM}|^2} + \Delta C_\mu}{\sqrt{|C_9^{\rm SM}|^2 + |C_{10}^{\rm SM}|^2} + \Delta C_e} \right)^2. \tag{72}$$

Taking into account that $C_9^{\rm SM} \approx -C_{10}^{\rm SM} \approx 4.1$, and the range for R_K in (65), we find in Fig. 7 the allowed region for the new physics deviations for muons and electrons, where the SM limit outside the region is shown. We must to compare the above region with the theoretical deviation, determined by the definition (71) and the parameters from (68). For convenience, we redefine some parameters. First, we define the effective flavor $U(1)_X$ coupling constants as:

$$(g_X^{(a)})^2 = g_X^2 K_9^{(a)}. \tag{73}$$

Second, we define the two ratios:

$$P_a = \frac{C_{10}^{NP(a)}}{C_9^{NP(a)}}, \qquad K_{21} = \frac{C_9^{NP(\mu)}}{C_9^{NP(e)}}. \tag{74}$$

Thus, the new physics contribution for the ninth electron Wilson coefficient is:

$$C_9^{NP(e)} = \frac{(g_X^{(e)})^2 (36\ \text{TeV})^2}{8 M_{Z'}^2}, \tag{75}$$

while all the remaining coefficients can be parametrized entirely as functions of this as:

$$C_9^{NP(\mu)} = K_{21} C_9^{NP(e)}, \qquad C_{10}^{NP(e)} = P_e C_9^{NP(e)},$$
$$C_{10}^{NP(\mu)} = P_\mu K_{21} C_9^{NP(e)}. \tag{76}$$

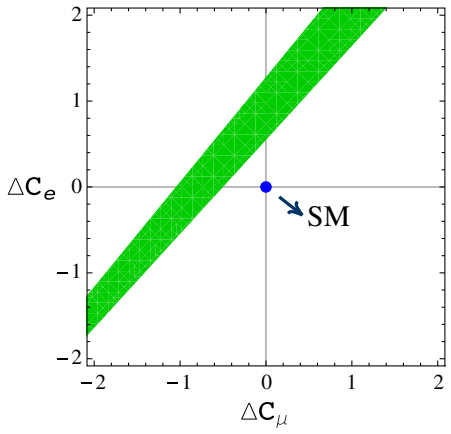

FIG. 7. Allowed region for the muon and electron new physics deviation defined as equation (71) compatible with the experimental data. The central blue point is the SM limit.

reducing the space of parameters to $(P_e, P_\mu, K_{21}, C_9^{NP(e)})$ which we must to fit in order to obtain the allowed deviations according to Fig. 7. Before doing this, we will show that the model predicts a relation between the parameters P_e and P_μ. We see from (68) and the definition in (69) that:

$$\frac{1 - P_e}{1 - P_\mu} = K_{21} \frac{|(V_L^E)_{31}|^2}{|(V_L^E)_{32}|^2}, \tag{77}$$

where $(V_L^E)_{3a}$ are the 31 and 32 components of the lepton left-handed matrix, that in the decoupling limit takes the form:

$$V_L^E = \begin{pmatrix} V_{\rm SM}^E & 0 \\ 0 & V_{\rm new}^E \end{pmatrix}, \tag{78}$$

with:

$$V_{\rm SM}^E = R(\theta_{23}^{E_L}) R(\theta_{13}^{E_L}) R(\theta_{12}^{E_L}), \tag{79}$$

where each rotation matrix $R(\theta)$ takes the same form as Eqs. (B5) for the quarks, and each angle is defined in (B14). In particular, we find for the 31 and 32 components that:

$$(V_L^E)_{31} = -s_{12}^{E_L}, \qquad (V_L^E)_{32} = c_{12}^{E_L}, \tag{80}$$

so that (77) become:

$$\frac{1 - P_e}{1 - P_\mu} = K_{21} |t_{12}^{E_L}|^2. \tag{81}$$

This condition is equivalent to:

$$(C_9^{NP(e)} - C_{10}^{NP(e)})/(C_9^{NP(\mu)} - C_{10}^{NP(\mu)}) = |t_{12}^{E_L}|^2. \tag{82}$$

According to (B28), the limit $t_{12}^{E_L} = 1$ is assumed in the natural parametrization. If in addition $P_e = -1$, we obtain for the new physics the same SM relation between the Wilson coefficients: $C_9^{NP(e)} = -C_{10}^{NP(e)}$. However, we did not find any allowed solution on this situation, as shown in graph (a) of Fig. 8, where the curves are the theoretical predictions for K_{21} ranging from 0 to very large values ($K_{21} \to \infty$). However, if we deviate from this scenario by choosing other values for P_e, we may fit the parameters into the anomaly region in the decoupling limit. For example, the graph (b) in the same figure displays the theoretical solutions for $P_e = -5$ where solutions into the allowed region are found in the interval $K_{21} = [1.2, 5]$. From the plot, we can estimate the bound $\Delta C_e \geq -2.6$ for the electron, while for the muon we obtain the allowed interval $-3.2 \leq \Delta C_\mu \leq -2.9$ when the former obtains its minimum value. Graph (c) shows the solutions for $P_e = 1$ for the interval $0 < K_{21} < 0.9$. Since K_{21} and $t_{12}^{E_L}$ are not zero,

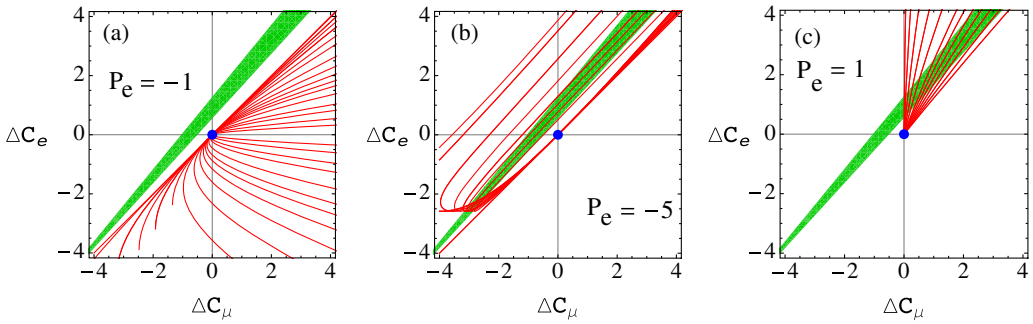

FIG. 8. New physics deviations of the Wilson coefficients for $t_{12}^{E_L} = 1$ and different values of P_e. In (a), there are not solutions through the allowed region for any value of K_{21}. In (b) and (c) solutions are found for $1.2 \leq K_{21} \leq 5$ and $0 < K_{21} \leq 0.9$, respectively. All the theoretical curves cross the SM limit (blue central point).

according to (82), this case also implies that $P_\mu = 1$. Thus, we found scenarios where $C_9^{NP(a)} = C_{10}^{NP(a)}$ for both $a = e$ and μ. In the limit $K_{21} \to 0$, corrections for the muon ΔC_μ does not exists, while for electron the allowed range according to graph (c) is $0.5 \leq \Delta C_e \leq 1.3$.

We also may explore scenarios with $t_{12}^{E_L} \neq 1$. In particular, the case with $P_e = -1$ can reproduce the reported data by properly fitting the other parameters, as shown in Fig. 9. In graph (a), we obtain solutions for the small ratio $K_{21} = 0.1$, and in the range $0 \leq t_{12}^{E_L} \leq 0.72$. Above this limit, the curves falls outside the allowed region, and $\Delta C_e = 0$ in the limit $t_{12}^{E_L} = 0$. We also see that the curves exhibits the bound $\Delta C_\mu \geq -1.8$. In the case with $K_{21} = 1$, graph (b) shows a larger range for the deviations, while allowed values extends to the bound $t_{12}^{E_L} < 1$. For the large value $K_{21} = 10$, the curves are shrunk again, as shown in graph (c), where $0 \leq t_{12}^{E_L} \leq 0.51$.

On the other hand, the ratio K_{21} also represents the relative coupling of e and μ to the Z' boson. Taking into account the Eqs. (68) and the definition (73), we obtain that:

$$K_{21} = \frac{C_9^{NP(\mu)}}{C_9^{NP(e)}} = \frac{(g_X^{(\mu)})^2}{(g_X^{(e)})^2}, \tag{83}$$

while the Wilson coefficient $C_9^{NP(e)}$ in Eq. (75) provides a relation between the effective electron coupling constant $g_X^{(e)}$ and the Z' mass. For example, the plot (a) in Fig. 10 shows the allowed regions of the electron Wilson coefficient for new physics as function of the ratio $K_{21} = C_9^{NP(\mu)}/C_9^{NP(e)}$, with $t_{12}^{E_L} = 1$ and different values of P_e: 0.2,0.5,1,2,5, and 10. The dashed horizontal line is the SM limit $C_9^{\mathrm{SM}} = 4.1$, where we can see that corrections can be smaller, at the same order or, eventually larger than the SM prediction. We see that $K_{21} < 1$, which means that solutions in this scenario are found if electrons couple stronger to the Z' boson than muons. Second, if $C_9^{NP(e)}$ increases, then P_e decreases in accordance with the definition $P_e = C_{10}^{NP(e)}/C_9^{NP(e)}$. So, we see in the plot that the lowest bounds are large for small values of P_e. Taking into account these bounds, the plot (b) displays the allowed region for the effective electron coupling $g_X^{(e)}$ and the Z' mass for a *muon-phobic* scenario with $K_{21} = 0$ ($g_X^{(\mu)} = 0$). The plot (c) shows the regions for $K_{21} = 0.53$, just at the upper limit of $P_e = 10$ as observed in plot (a), and described by the green dashed line in (c). The conversion to the muon coupling is obtained by doing $g_X^{(e)} \times \sqrt{0.53}$, according to (83). In general, we see that large ratios P_e

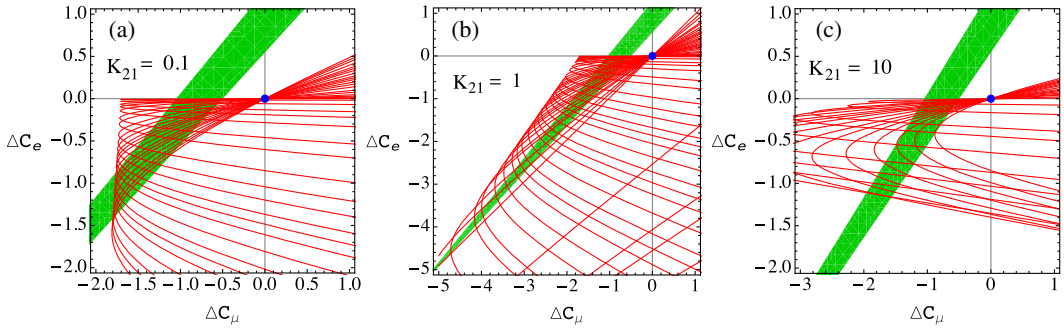

FIG. 9. New physics deviations of the Wilson coefficients for $P_e = -1$ and (a) $K_{21} = 0.1$, (b) 1 and (c) 10. The curves are for different ranges of $t_{12}^{E_L}$.

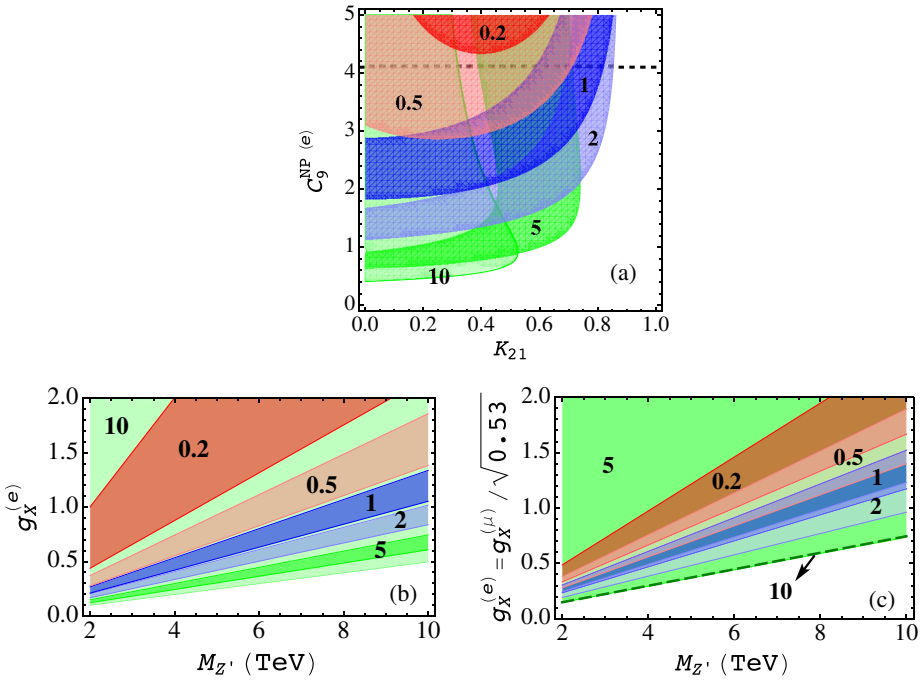

FIG. 10. Figure (a) shows allowed regions in the $(C_9^{NP(e)}, K_{21})$ plane for $P_e = 0.2$, 0.5, 1, 2, 5 and 10. For reference, the dashed horizontal line is the SM limit $C_9^{\mathrm{SM}} = 4.1$. The plot (b) is the effective coupling as function of the Z' boson mass according to regions in (a) for $K_{21} = 0$. Figure (c) is for $K_{21} = 0.53$.

favor regions including small gauge couplings constants, which increase as the Z' boson become heavier.

V. CONCLUSIONS

Observational facts as the fermion mass hierarchies, mixing schemes, oscillation of neutrinos and experimental anomalies as the B meson decay may be manifestations of new physics beyond the SM. Motivated initially by the fermion mass hierarchy problem, we propose a nonuniversal $U(1)'$ extension with three Higgs doublets that may reproduce masses and mixing schemes for quarks, charged and neutral leptons. In addition to new charged and neutral Higgs particles, the model introduces other particles from the following conditions:

(1) Due to the new abelian gauge symmetry, a second neutral gauge boson Z' is naturally introduced.
(2) In order to break the $U(1)'$ symmetry and provide mass to the Z' boson, a new Higgs singlet with large VEV is added.
(3) Also, the new Z' gauge boson induces chiral anomalies, which may spoil the renormalization of the model. In order to restore the cancellation of these anomalies, we must assign suitable $U(1)'$ charges to the fermions. This assignation is done to obtain flavor nonuniversal interactions for quarks and leptons, which requires extra quarks and charged leptons.

The model exhibits lepton universality violation that may explain the B meson decay anomaly into electron and muon pairs reported by the LHCb collaboration. This observable may test the new couplings of the model, in particular, the anomaly is highly sensitive to the new quark and lepton content of the model through their couplings with the Higgs sector. They participate in the meson decay indirectly through their mixing couplings with the ordinary quarks b and s, and the charged leptons e and μ. Since these mixings occur in a nonuniversal form, then the anomaly can be explained and fitted for new physics at the TeV scale, attainable to be proved in the LHC.

Although we choose an specific scheme to parameterize the mass matrices for fermions and the mixing angles, they are suppressed or enhanced by ratios of VEVs which we preserve in the natural scheme. Specifically, the VEV of the first Higgs doublet determine the scale of the top quark, i.e., $v_1/\sqrt{2} \sim 173$ GeV. The second VEV gives masses to the quark b and the lepton τ at $v_2/\sqrt{2} \sim 3$ GeV. Finally, the third VEV is of the order of the quark s and lepton μ mass, at $v_3/\sqrt{2} \sim 0.1$ GeV. Thus, we expect mixing angles with values of the order of the ratios of the phenomenological fermions measured experimentally independent of the chosen scheme to address the Yukawa free parameters.

ACKNOWLEDGMENTS

This work was supported by *El Patrimonio Autonomo Fondo Nacional de Financiamiento para la Ciencia, la Tecnología y la Innovación Francisco José de Caldas* programme of COLCIENCIAS in Colombia. R. M. thanks

to professor Germán Valencia for the kind hospitality at Monash University and his useful comments.

APPENDIX A: BLOCK DIAGONALIZATION

Let us take a generic matrix with arbitrary dimension of the form:

$$M^2 = \begin{pmatrix} A & C \\ C^T & D \end{pmatrix}, \tag{A1}$$

with A, D, and C submatrices whose elements obey the hierarchy

$$A \ll C \ll D. \tag{A2}$$

The matrix (A1), as shown in Ref. [17], can be block diagonalized approximately by a unitary rotation of the form:

$$V = \begin{pmatrix} I & F \\ -F^T & I \end{pmatrix}, \tag{A3}$$

where I is an identity matrix, and F a small subrotation with $F \ll 1$. Keeping only up to linear terms on F, the rotation gives:

$$V^T M^2 V = \begin{pmatrix} A - CF^T - FC^T & C + AF - FD \\ C^T + F^T A - DF^T & D + C^T F + F^T C \end{pmatrix}, \tag{A4}$$

which, by definition, must lead us to a diagonal block form

$$m^2 = \begin{pmatrix} a & 0 \\ 0 & d \end{pmatrix}, \tag{A5}$$

with a and d nondiagonal matrices, and 0 the null matrix. By matching the upper right nondiagonal block in (A4) and (A5), we obtain that $C + AF - FD = 0$. Taking into account the hierarchy in (A2), we may neglect the term with A, finding the following approximate solution:

$$F \approx CD^{-1}. \tag{A6}$$

On the other hand, if we match the diagonal blocks in (A4) and (A5), and using the solution (A6), we can obtain the form of the submatrices a and b in terms of the original blocks A, C, and D. We obtain at dominant order that:

$$\begin{aligned} a &\approx A - CD^{-1}C^T \\ b &\approx D. \end{aligned} \tag{A7}$$

The above matrices can be diagonalized independently.

APPENDIX B: PARAMETRIZATION OF THE BIUNITARY MATRIX TRANSFORMATIONS

In this Appendix we obtain the parameters of the biunitary transformations that rotate the flavor fermion basis into mass basis.

1. Up sector

From the Yukawa Lagrangian (3), we obtain the following mass matrix for the up-type quark sector:

$$\mathbb{M}_U = \frac{1}{\sqrt{2}} \begin{pmatrix} h^{11}_{3u} v_3 & h^{12}_{2u} v_2 & h^{13}_{3u} v_3 & h^{1}_{2\mathcal{T}} v_2 \\ 0 & h^{22}_{1u} v_1 & 0 & h^{2}_{1\mathcal{T}} v_1 \\ h^{31}_{1u} v_1 & 0 & h^{33}_{1u} v_1 & 0 \\ 0 & g^{2}_{\chi u} v_\chi & 0 & g_{\chi\mathcal{T}} v_\chi \end{pmatrix}, \tag{B1}$$

which diagonalizes through the biunitary matrices $V^U_{L(R)}$. In particular, as shown in Ref. [14], the left-handed matrix can be expressed as the product of two mixing matrices of the form:

$$V^U_L = \begin{pmatrix} 1 & \Theta^{U\dagger}_L \\ -\Theta^U_L & 1 \end{pmatrix} \begin{pmatrix} V^U_{\rm SM} & 0 \\ 0 & V^U_{\rm new} \end{pmatrix}, \tag{B2}$$

where Θ^U_L is a seesaw matrix that block-diagonalize the mass matrix into one mass matrix of the ordinary SM quarks and a heavy matrix that mixes the new quarks, while $V^U_{\rm SM}$ and $V^U_{\rm new}$ diagonalize each of these matrices. For simplicity, we assume diagonal exotic matrices, so that $V^f_{\rm new} = 1$. The seesaw matrix is

$$\Theta^{U\dagger}_L = \begin{pmatrix} \frac{h^1_{2\mathcal{T}} g_{\chi\mathcal{T}} + h^{12}_{2u} g^2_{\chi u}}{(g_{\chi\mathcal{T}})^2 + (g^2_{\chi u})^2} \frac{v_2}{v_\chi} \\ \frac{h^2_{1\mathcal{T}} g_{\chi\mathcal{T}} + h^{22}_{1u} g^2_{\chi u}}{(g_{\chi\mathcal{T}})^2 + (g^2_{\chi u})^2} \frac{v_1}{v_\chi} \\ 0 \end{pmatrix}, \tag{B3}$$

and the SM matrix has the form:

$$V^U_{\rm SM} = R_{23}(\theta^U_{23}) R_{13}(\theta^U_{13}) R_{12}(\theta^U_{12}), \tag{B4}$$

with

$$R_{12}(\theta^U_{12}) = \begin{pmatrix} c^U_{12} & s^U_{12} & 0 \\ -s^U_{12} & c^U_{12} & 0 \\ 0 & 0 & 1 \end{pmatrix}, \tag{B5a}$$

$$R_{13}(\theta^U_{13}) = \begin{pmatrix} c^U_{13} & 0 & s^U_{13} \\ 0 & 1 & 0 \\ -s^U_{13} & 0 & c^U_{13} \end{pmatrix}, \tag{B5b}$$

$$R_{23}(\theta^U_{23}) = \begin{pmatrix} 1 & 0 & 0 \\ 0 & c^U_{23} & s^U_{23} \\ 0 & -s^U_{23} & c^U_{23} \end{pmatrix}, \tag{B5c}$$

and $c_{ij}^U = \cos\theta_{ij}^U$ and $s_{ij}^U = \sin\theta_{ij}^U$. The angles θ_{ij}^U are specified by their tangents $t_{ij}^U = \tan\theta_{ij}^U$, which are [14]

$$t_{12}^U = \frac{h_{2u}^{12} g_{\chi\mathcal{T}} - h_{2\mathcal{T}}^{1} g_{\chi u}^{2}}{h_{1u}^{22} g_{\chi\mathcal{T}} - h_{1\mathcal{T}}^{2} g_{\chi u}^{2}} \frac{v_2}{v_1},$$
$$t_{13}^U = \frac{h_{3u}^{13} h_{1u}^{33} + h_{3u}^{11} h_{1u}^{31}}{(h_{1u}^{33})^2 + (h_{1u}^{31})^2} \frac{v_3}{v_1}, \quad t_{23}^U = 0. \tag{B6}$$

Finally, the squared mass eigenvalues are

$$m_u^2 = \frac{(h_{3u}^{11} h_{1u}^{33} - h_{3u}^{13} h_{1u}^{31})^2}{(h_{1u}^{33})^2 + (h_{1u}^{31})^2} \frac{v_3^2}{2},$$
$$m_c^2 = \frac{(h_{1u}^{22} g_{\chi\mathcal{T}} - h_{1\mathcal{T}}^{2} g_{\chi u}^{2})^2}{(g_{\chi\mathcal{T}})^2 + (g_{\chi u}^{2})^2} \frac{v_1^2}{2},$$
$$m_t^2 = [(h_{1u}^{33})^2 + (h_{1u}^{31})^2] \frac{v_1^2}{2},$$
$$m_T^2 = [(g_{\chi\mathcal{T}})^2 + (g_{\chi u}^{2})^2] \frac{v_\chi^2}{2}. \tag{B7}$$

2. Down sector

The mass matrix of the down-type quarks is

$$\mathbb{M}_D = \frac{1}{\sqrt{2}} \begin{pmatrix} \Sigma_d^{11} & \Sigma_d^{12} & \Sigma_d^{13} & h_{1\mathcal{J}}^{11} v_1 & h_{1\mathcal{J}}^{12} v_1 \\ h_{3d}^{21} v_3 & h_{3d}^{22} v_3 & h_{3d}^{23} v_3 & h_{2\mathcal{J}}^{21} v_2 & h_{2\mathcal{J}}^{22} v_2 \\ h_{2d}^{31} v_2 & h_{2d}^{32} v_2 & h_{2d}^{33} v_2 & h_{3\mathcal{J}}^{31} v_3 & h_{3\mathcal{J}}^{32} v_3 \\ 0 & 0 & 0 & g_{\chi\mathcal{J}}^{1} v_\chi & 0 \\ 0 & 0 & 0 & 0 & g_{\chi\mathcal{J}}^{2} v_\chi \end{pmatrix}, \tag{B8}$$

where Σ_d^{1k} are one-loop mass components. The see-saw matrix is

$$\Theta_L^{D\dagger} = \begin{pmatrix} \frac{h_{1\mathcal{J}}^{11}}{g_{\chi\mathcal{J}}^{1}} \frac{v_1}{v_\chi} & \frac{h_{1\mathcal{J}}^{12}}{g_{\chi\mathcal{J}}^{2}} \frac{v_1}{v_\chi} \\ \frac{h_{2\mathcal{J}}^{21}}{g_{\chi\mathcal{J}}^{1}} \frac{v_2}{v_\chi} & \frac{h_{2\mathcal{J}}^{22}}{g_{\chi\mathcal{J}}^{2}} \frac{v_2}{v_\chi} \\ \frac{h_{3\mathcal{J}}^{31}}{g_{\chi\mathcal{J}}^{1}} \frac{v_3}{v_\chi} & \frac{h_{3\mathcal{J}}^{32}}{g_{\chi\mathcal{J}}^{2}} \frac{v_3}{v_\chi} \end{pmatrix}, \tag{B9}$$

and the SM angles of $\mathbb{V}_{L,\mathrm{B}}^D$ are given by

$$t_{12}^D = \frac{\Sigma_d^{11} h_{3d}^{21} + \Sigma_d^{12} h_{3d}^{22} + \Sigma_d^{13} h_{3d}^{23}}{(h_{3d}^{21})^2 + (h_{3d}^{22})^2 + (h_{3d}^{23})^2} \frac{1}{v_3}, \quad t_{13}^D = \frac{\Sigma_d^{11} h_{2d}^{31} + \Sigma_d^{12} h_{2d}^{32} + \Sigma_d^{13} h_{2d}^{33}}{(h_{2d}^{31})^2 + (h_{2d}^{32})^2 + (h_{2d}^{33})^2} \frac{1}{v_2}, \quad t_{23}^D = \frac{h_{3d}^{21} h_{2d}^{31} + h_{3d}^{22} h_{2d}^{32} + h_{3d}^{23} h_{2d}^{33}}{(h_{2d}^{31})^2 + (h_{2d}^{32})^2 + (h_{2d}^{33})^2} \frac{v_3}{v_2}, \tag{B10}$$

while the mass eigenvalues are

$$m_d^2 = \frac{[(\Sigma_d^{11} h_{3d}^{22} - \Sigma_d^{12} h_{3d}^{21}) h_{2d}^{33} + (\Sigma_d^{13} h_{3d}^{21} - \Sigma_d^{11} h_{3d}^{23}) h_{2d}^{32} + (\Sigma_d^{12} h_{3d}^{23} - \Sigma_d^{13} h_{3d}^{22}) h_{2d}^{31}]^2}{[(h_{3d}^{21})^2 + (h_{3d}^{22})^2](h_{2d}^{33})^2 + [(h_{3d}^{23})^2 + (h_{3d}^{21})^2](h_{2d}^{32})^2 + [(h_{3d}^{22})^2 + (h_{3d}^{23})^2](h_{2d}^{31})^2},$$
$$m_s^2 = \frac{[(h_{3d}^{21})^2 + (h_{3d}^{22})^2](h_{2d}^{33})^2 + [(h_{3d}^{23})^2 + (h_{3d}^{21})^2](h_{2d}^{32})^2 + [(h_{3d}^{22})^2 + (h_{3d}^{23})^2](h_{2d}^{31})^2}{(h_{2d}^{33})^2 + (h_{2d}^{32})^2 + (h_{2d}^{31})^2} \frac{v_3^2}{2},$$
$$m_b^2 = [(h_{2d}^{33})^2 + (h_{2d}^{32})^2 + (h_{2d}^{31})^2] \frac{v_2^2}{2},$$
$$m_{J1}^2 = (g_{\chi\mathcal{J}}^{1})^2 \frac{v_\chi^2}{2}, m_{J2}^2 = (g_{\chi\mathcal{J}}^{2})^2 \frac{v_\chi^2}{2}. \tag{B11}$$

3. Charged lepton sector: Left-handed

The mass matrix of the charged leptons is

$$\mathbb{M}_E = \frac{1}{\sqrt{2}} \begin{pmatrix} 0 & h_{3e}^{e\mu} v_3 & 0 & h_{1\mathcal{E}}^{e1} v_1 & 0 \\ 0 & h_{3e}^{\mu\mu} v_3 & 0 & h_{1\mathcal{E}}^{\mu 1} v_1 & 0 \\ h_{2e}^{\tau e} v_2 & 0 & h_{2e}^{\tau\tau} v_2 & 0 & 0 \\ g_{\chi e}^{1e} v_\chi & 0 & 0 & g_{\chi\mathcal{E}}^{1} v_\chi & 0 \\ 0 & g_{\chi e}^{2\mu} v_\chi & 0 & 0 & g_{\chi\mathcal{E}}^{2} v_\chi \end{pmatrix}, \tag{B12}$$

with left-handed matrix rotations:

$$\Theta_L^{E\dagger} = \begin{pmatrix} \frac{h_{1\mathcal{E}}^{e1} g_{\chi\mathcal{E}}^{1} v_1 v_\chi}{2 m_{E^2}^2} & \frac{h_{3e}^{e\mu} g_{\chi e}^{2\mu} v_3 v_\chi}{2 m_{E^1}^2} \\ \frac{h_{1\mathcal{E}}^{\mu 1} g_{\chi\mathcal{E}}^{1} v_1 v_\chi}{2 m_{E^2}^2} & \frac{h_{3e}^{\mu\mu} g_{\chi e}^{2\mu} v_3 v_\chi}{2 m_{E^2}^2} \\ \frac{h_{3e}^{e\mu} g_{\chi e}^{1e} v_3 v_\chi}{2 m_{E^2}^2} & 0 \end{pmatrix}, \tag{B13}$$

and

$$t_{12}^{E_L} \approx \frac{h_{1\mathcal{E}}^{e1}}{h_{1\mathcal{E}}^{\mu 1}}, \quad t_{13}^{E_L} \approx \frac{g_{\chi\mathcal{E}}^{1} h_{3e}^{e\mu}}{g_{\chi e}^{1e} h_{1\mathcal{E}}^{e1}} \frac{v_3}{v_1},$$
$$t_{23}^{E_L} \approx -\frac{2(g_{\chi\mathcal{E}}^{1})^3 h_{3e}^{e\mu} (h_{2e}^{\tau\tau})^2}{(g_{\chi e}^{1e})^3 h_{1\mathcal{E}}^{\mu 1} (h_{1\mathcal{E}}^{e1})^2} \frac{v_2^2 v_3}{v_1^3}. \tag{B14}$$

The mass values are

$$m_e^2 = \frac{(h_{3e}^{e\mu} h_{1\mathcal{E}}^{\mu 1} - h_{3e}^{\mu\mu} h_{1\mathcal{E}}^{e1})^2}{(h_{1\mathcal{E}}^{e1})^2 + (h_{1\mathcal{E}}^{\mu 1})^2} \frac{v_3^2}{2},$$
$$m_\mu^2 = \frac{(h_{3e}^{e\mu} h_{1\mathcal{E}}^{e1} + h_{3e}^{\mu\mu} h_{1\mathcal{E}}^{\mu 1})^2}{(h_{1\mathcal{E}}^{e1})^2 + (h_{1\mathcal{E}}^{\mu 1})^2} \frac{v_3^2}{2} + \frac{(h_{3e}^{e\mu})^2 v_3^2}{2},$$
$$m_\tau^2 = (h_{2e}^{\tau\tau})^2 \frac{v_2^2}{2},$$
$$m_{E1}^2 = [(g_{\chi\mathcal{E}}^{1})^2 + (g_{\chi e}^{1e})^2] \frac{v_\chi^2}{2},$$
$$m_{E2}^2 = [(g_{\chi\mathcal{E}}^{2})^2 + (g_{\chi e}^{2\mu})^2] \frac{v_\chi^2}{2}. \tag{B15}$$

4. Charged lepton sector: Right-handed

In addition, we need the rotations for the right-handed components of the charged leptons. To obtain these parameters, we must construct the squared mass matrix $\mathbb{M}_R^E = \mathbb{M}_E^\dagger \mathbb{M}_E$, which is diagonalized by the right-handed transformation V_R^E. In this case, the rotation matrix is expressed as:

$$V_R^E = \begin{pmatrix} \Theta_{R11}^E & \Theta_{R12}^{ET} \\ \Theta_{R21}^E & \Theta_{R22}^E \end{pmatrix} \begin{pmatrix} V_{\mathrm{SM}}^{E_R} & 0 \\ 0 & V_{\mathrm{new}}^{E_R} \end{pmatrix}, \tag{B16}$$

with:

$$\Theta_{R11}^E = \begin{pmatrix} c_{14}^{E_R} & 0 & 0 \\ 0 & c_{25}^{E_R} & 0 \\ -s_{34}^{E_R} s_{14}^{E_R} & 0 & c_{34}^{E_R} \end{pmatrix}$$
$$\Theta_{R12}^E = \begin{pmatrix} s_{14}^{E_R} & 0 & s_{34}^{E_R} c_{14}^{E_R} \\ 0 & s_{25}^{E_R} & 0 \end{pmatrix}$$
$$\Theta_{R21}^E = \begin{pmatrix} -c_{34}^{E_R} s_{14}^{E_R} & 0 & -s_{34}^{E_R} \\ 0 & -s_{25}^{E_R} & 0 \end{pmatrix}$$
$$\Theta_{R22}^E = \begin{pmatrix} c_{34}^{E_R} c_{14}^{E_R} & 0 \\ 0 & c_{25} \end{pmatrix}, \tag{B17}$$

where the tangent of the mixing angles are

$$t_{25}^{E_R} = \frac{g_{\chi e}^{2\mu}}{g_{\chi\mathcal{E}}^{2}}, \quad t_{34}^{E_R} = \frac{g_{\chi e}^{1e}}{g_{\chi\mathcal{E}}^{1}},$$
$$t_{14}^{E_R} = \frac{g_{\chi e}^{1e}}{\sqrt{(g_{\chi\mathcal{E}}^{1})^2 + (g_{\chi e}^{1e})^2}}, \tag{B18}$$

while the SM mixing angles are

$$t_{12}^{E_R} = -\frac{g_{\chi e}^{1e}[(h_{1\mathcal{E}}^{e1})^2 + (h_{1\mathcal{E}}^{\mu 1})^2]}{g_{\chi\mathcal{E}}^{1}(h_{1\mathcal{E}}^{e1} h_{3e}^{e\mu} + h_{1\mathcal{E}}^{\mu 1} h_{3e}^{\mu\mu})} \frac{v_1}{v_3},$$
$$t_{23}^{E_R} = \frac{g_{\chi\mathcal{E}}^{1} h_{2e}^{\tau e} (h_{1\mathcal{E}}^{e1} h_{3e}^{e\mu} + h_{1\mathcal{E}}^{\mu 1} h_{3e}^{\mu\mu})}{g_{\chi e}^{1e} h_{2e}^{\tau\tau}[(h_{1\mathcal{E}}^{e1})^2 + (h_{1\mathcal{E}}^{\mu 1})^2]} \frac{v_3^2}{v_1 v_2},$$
$$t_{13}^{E_R} = \frac{(g_{\chi\mathcal{E}}^{1})^2 h_{2e}^{\tau e} h_{2e}^{\tau\tau}}{(g_{\chi e}^{1e})^2[(h_{1\mathcal{E}}^{e1})^2 + (h_{1\mathcal{E}}^{\mu 1})^2]} \frac{v_2 v_3}{v_1^2}. \tag{B19}$$

5. Natural parametrization

In order to simplify the analysis, we separate the Yukawa interactions in three parts. First, the couplings among the ordinary SM fermions. Second, the interactions among the new particle content. Finally, the mixing couplings of the ordinary and the new particles. We assume a "natural" limit, where each part couple independently with the same strength. As a consequence, the mass matrices shares Yukawa couplings in some components. For example, in the up-type sector, by calling $h_{ku}^{ij} = h_u$, $g_{\chi\mathcal{T}} = g_{\mathcal{T}}$, $h_{i\mathcal{T}}^{j} = h_{\mathcal{T}}$ and $g_{\chi u}^{2} = g_u$, the mass matrix in (B1) become:

$$\mathbb{M}_U = \frac{1}{\sqrt{2}} \begin{pmatrix} h_u v_3 & h_u v_2 & h_u v_3 & h_{\mathcal{T}} v_2 \\ 0 & h_u v_1 & 0 & h_{\mathcal{T}} v_1 \\ h_u v_1 & 0 & h_u v_1 & 0 \\ 0 & g_u v_\chi & 0 & g_{\mathcal{T}} v_\chi \end{pmatrix}. \tag{B20}$$

In particular, in this limit, the mass of the top quark is

$$m_t^2 = h_u^2 v_1^2, \tag{B21}$$

from where we obtain the VEV of the first Higgs triplet, $v_1 = m_t/h_u$. In the same form, the down-type mass matrix in (B8) is written as

$$\mathbb{M}_D = \frac{1}{\sqrt{2}} \begin{pmatrix} \Sigma_d^{11} & \Sigma_d^{12} & \Sigma_d^{13} & h_{\mathcal{J}} v_1 & h_{\mathcal{J}} v_1 \\ h_d v_3 & h_d v_3 & h_d v_3 & h_{\mathcal{J}} v_2 & h_{\mathcal{J}} v_2 \\ h_d v_2 & h_d v_2 & h_d v_2 & h_{\mathcal{J}} v_3 & h_{\mathcal{J}} v_3 \\ 0 & 0 & 0 & g_{\mathcal{J}} v_\chi & 0 \\ 0 & 0 & 0 & 0 & g_{\mathcal{J}} v_\chi \end{pmatrix}. \tag{B22}$$

In this case, the masses of the quarks are

$$m_d^2 \sim \Sigma_d, \quad m_s^2 = h_d^2 v_3^2,$$
$$m_b^2 = \frac{3}{2} h_d^2 v_2^2, \quad m_J^2 = \frac{1}{2} g_{\mathcal{J}}^2 v_\chi^2, \tag{B23}$$

from where we obtain the VEVs for the other two Higgs triplets and the singlet as functions of the quarks masses: $v_2 = \sqrt{2} m_b/\sqrt{3} h_d$, $v_3 = m_s/h_d$, and $v_\chi = \sqrt{2} m_J/g_{\mathcal{J}}$. With this scheme, the mixing angles (B9) and (B10) can be parametrized as:

$$\Theta_L^{D\dagger} = \frac{h_{\mathcal{J}}}{h_u} \begin{pmatrix} \frac{1}{\sqrt{2}}\frac{m_t}{m_J} & \frac{1}{\sqrt{2}}\frac{m_t}{m_J} \\ \frac{1}{\sqrt{3}}\frac{m_b}{m_J}\frac{h_u}{h_d} & \frac{1}{\sqrt{3}}\frac{m_b}{m_J}\frac{h_u}{h_d} \\ \frac{1}{\sqrt{3}}\frac{m_s}{m_J}\frac{h_u}{h_d} & \frac{1}{\sqrt{3}}\frac{m_s}{m_J}\frac{h_u}{h_d} \end{pmatrix}, \tag{B24}$$

and

$$t_{12}^D = \frac{m_d}{m_s} \quad t_{13}^D = \frac{\sqrt{3}}{\sqrt{2}}\frac{m_d}{m_b} \quad t_{23}^D = \frac{\sqrt{3}}{\sqrt{2}}\frac{m_s}{m_b}. \tag{B25}$$

We see that the mixing matrix (B24) depends on the ratio $r_{\mathcal{J}} = h_{\mathcal{J}}/h_u$.

Regarding the lepton sector, the mass matrix (B12) simplify to:

$$\mathbb{M}_E = \frac{1}{\sqrt{2}} \begin{pmatrix} 0 & h_e v_3 & 0 & h_{\mathcal{E}} v_1 & 0 \\ 0 & h_e v_3 & 0 & h_{\mathcal{E}} v_1 & 0 \\ h_e v_2 & 0 & h_e v_2 & 0 & 0 \\ g_e v_\chi & 0 & 0 & g_{\mathcal{E}} v_\chi & 0 \\ 0 & g_e v_\chi & 0 & 0 & g_{\mathcal{E}} v_\chi \end{pmatrix}, \tag{B26}$$

from where the charged lepton masses are expressed as:

$$m_e^2 \approx 0, \quad m_\mu^2 = \frac{3}{2} h_e^2 v_3^2,$$
$$m_\tau^2 = \frac{1}{2} h_e^2 v_2^2 \quad m_E^2 = [(g_e)^2 + (g_{\mathcal{E}})^2] \frac{v_\chi^2}{2}. \tag{B27}$$

Thus, the VEVs, in this case, can be written in terms of the lepton couplings as $v_2 = \sqrt{2} m_\tau/h_e$, $v_3 = \sqrt{2} m_\mu/\sqrt{3} h_e$ and $v_\chi = \sqrt{2} m_E/\sqrt{(g_e)^2 + (g_{\mathcal{E}})^2}$.

For the mixing angles, we choose two of them as free parameters. For the left-handed angles in (B14), we choose $t_{13}^{E_L}$ as a free parameter, while for the right-handed angles in (B18) we take $t_{25}^{E_R}$. Thus, with the natural parametrization, the other mixing angles are

$$t_{12}^{E_L} \approx 1, \quad t_{23}^{E_L} \approx -\frac{6 m_\tau^2}{m_\mu^2} (t_{13}^{E_L})^3,$$
$$t_{12}^{E_R} \approx -\frac{1}{t_{13}^{E_L}}, \quad t_{23}^{E_R} \approx \frac{m_\mu}{\sqrt{3} m_\tau} t_{13}^{E_L},$$
$$t_{13}^{E_R} \approx \frac{3 m_\tau}{2 m_\mu} (t_{13}^{E_L})^2, \quad t_{34}^{E_R} \approx t_{25}^{E_R}, \quad t_{14}^{E_R} \approx s_{25}^{E_R}, \tag{B28}$$

while the mixing matrix (B13) takes the form:

$$\Theta_L^{E\dagger} = \frac{h_{\mathcal{E}}}{h_u} \begin{pmatrix} \frac{1}{\sqrt{2}}\frac{m_t}{m_E} c_{25}^{E_R} & \frac{m_\mu}{m_E}\frac{h_{\mathcal{E}}}{\sqrt{3} h_u} s_{25}^{E_R} \\ \frac{1}{\sqrt{2}}\frac{m_t}{m_E} c_{25}^{E_R} & \frac{m_\mu}{m_E}\frac{h_{\mathcal{E}}}{\sqrt{3} h_u} s_{25}^{E_R} \\ \frac{m_\mu}{m_E}\frac{h_{\mathcal{E}}}{\sqrt{3} h_u} s_{25}^{E_R} & 0 \end{pmatrix}, \tag{B29}$$

We also see that the above matrix is function of the ratio $r_{\mathcal{E}} = h_{\mathcal{E}}/h_u$.

Putting all the above matrices together, we will obtain each component of the original biunitary transformations V_L^D, V_L^E, and V_R^E. In particular, the neutral current couplings for electrons depends on $(V_L^E)_{31,41,51}$ and $(V_R^E)_{21,41,51}$, while for muons we need $(V_L^E)_{32,42,52}$ and $(V_R^E)_{22,42,52}$. They are

$$(V_L^E)_{51,(52)} = 0$$
$$(V_L^E)_{31,(32)} = \frac{-t_{13}^{E_L}}{\sqrt{2}\sqrt{1 + 36 x^4 (t_{13}^{E_L})^6}} [c_{13}^{E_L} \pm 6 x^2 (t_{13}^{E_L})^2]$$
$$(V_L^E)_{41,(42)} = \frac{-1}{2} y r_{\mathcal{E}} c_{25}^{E_R} \left[s_{13}^{E_L} + \frac{\mp 1 + 6 x^2 c_{13}^{E_L} (t_{13}^{E_L})^4}{\sqrt{1 + 36 x^4 (t_{13}^{E_L})^6}} \right], \tag{B30}$$

where $x = m_\tau/m_\mu$ and $y = m_t/m_E$, and:

$$
\begin{aligned}
(V_R^E)_{21} &= -t_{25}^{E_R}(V_R^E)_{51} = \frac{c_{13}^{E_L}c_{25}^{E_R}}{\sqrt{1+\frac{1}{3x^2}(t_{13}^{E_L})^2}}\left[1-\frac{\sqrt{3}(t_{13}^{E_L})^4}{2\sqrt{1+\frac{9}{4}x^2(t_{13}^{E_L})^4}}\right]\\
(V_R^E)_{22} &= -t_{25}^{E_R}(V_R^E)_{52} = \frac{s_{13}^{E_L}c_{25}^{E_R}}{\sqrt{1+\frac{1}{3x^2}(t_{13}^{E_L})^2}}\left[1+\frac{\sqrt{3}(t_{13}^{E_L})^2}{2\sqrt{1+\frac{9}{4}x^2(t_{13}^{E_L})^4}}\right],\\
(V_R^E)_{41} &= \frac{s_{13}^{E_L}s_{25}^{E_R}}{\sqrt{3}x\sqrt{1+\frac{1}{3x^2}(t_{13}^{E_L})^2}}+\frac{3s_{13}^{E_L}(t_{13}^{E_L})^2s_{25}^{E_R}x}{2\sqrt{1+\frac{9}{4}x^2(t_{13}^{E_L})^4}}\left[\frac{1}{\sqrt{1+\frac{1}{3x^2}(t_{13}^{E_L})^2}}-\frac{c_{25}^{E_R}}{\sqrt{1+(s_{25}^{E_R})^2}}\right]\\
(V_R^E)_{42} &= \frac{s_{13}^{E_L}s_{25}^{E_R}t_{13}^{E_L}}{\sqrt{3}x\sqrt{1+\frac{1}{3x^2}(t_{13}^{E_L})^2}}+\frac{3s_{13}^{E_L}t_{13}^{E_L}s_{25}^{E_R}x}{2\sqrt{1+\frac{9}{4}x^2(t_{13}^{E_L})^4}}\left[\frac{-1}{\sqrt{1+\frac{1}{3x^2}(t_{13}^{E_L})^2}}+\frac{c_{25}^{E_R}}{\sqrt{1+(s_{25}^{E_R})^2}}\right]
\end{aligned}
\tag{B31}
$$

[1] S. L. Glashow, Nucl. Phys. **22**, 579 (1961); S. Weinberg, Phys. Rev. Lett. **19**, 1264 (1967); A. Salam, in *Elementary Particle Theory: Relativistic Groups and Analyticity (Nobel Symposium No. 8)*, edited by N. Svartholm (Almqvist and Wiksell, Stockholm, 1968), p. 367.

[2] H. Georgi, Phys. Lett. **169B**, 231 (1986).

[3] T. Yanagida, Prog. Theor. Phys. **64**, 1103 (1980); R. N. Mohapatra and G. Senjanovic, Phys. Rev. Lett. **44**, 912 (1980); J. Schechter and J. W. Valle, Phys. Rev. D **22**, 2227 (1980); R. N. Mohapatra, Phys. Rev. Lett. **56**, 561 (1986); R. N. Mohapatra and J. W. Valle, Phys. Rev. D **34**, 1642 (1986); E. Cataño, R. Martinez, and F. Ochoa, Phys. Rev. D **86**, 073015 (2012); A. G. Dias, C. d. S. Pires, P. R. da Silva, and A. Sampieri, Phys. Rev. D **86**, 035007 (2012).

[4] R. Aaij *et al.* (LHCb Collaboration), Phys. Rev. Lett. **111**, 191801 (2013); J. High Energy Phys. 06 (2014) 133; 07 (2013) 084; 04 (2015) 064.

[5] J. Matias, F. Mescia, M. Ramon, and J. Virto, J. High Energy Phys. 04 (2012) 104; S. Descotes-Genon, J. Matias, and J. Virto, Phys. Rev. D **88**, 074002 (2013); W. Altmannshofer and D. M. Straub, Eur. Phys. J. C **73**, 2646 (2013); T. Hurth and F. Mahmoudi, J. High Energy Phys. 04 (2014) 097; F. Mahmoudi, S. Neshatpour, and J. Virto, Eur. Phys. J. C **74**, 2927 (2014); T. Hurth, F. Mahmoudi, and S. Neshatpour, J. High Energy Phys. 12 (2014) 053; S. Jager and J. Martin Camalich, J. High Energy Phys. 05 (2013) 043; G. Hiller and M. Schmaltz, Phys. Rev. D **90**, 054014 (2014); A. J. Buras, F. De Fazio, and J. Girrbach, J. High Energy Phys. 02 (2014) 112; A. J. Buras, F. De Fazio, and J. Girrbach-Noe, J. High Energy Phys. 08 (2014) 039; R. Gauld, F. Goertz, and U. Haisch, J. High Energy Phys. 01 (2014) 069; R. Gauld, F. Goertz, and U. Haisch, Phys. Rev. D **89**, 015005 (2014); E. Lunghi and J. Matias, J. High Energy Phys. 04 (2007) 058; W. Altmannshofer, P. Ball, A. Bharucha, A. J. Buras, D. M. Straub, and M. Wick, J. High Energy Phys. 01 (2009) 019; A. Crivellin, G. D'Ambrosio, and J. Heeck, Phys. Rev. Lett. **114**, 151801 (2015); Phys. Rev. D **91**, 075006 (2015); A. Crivellin, L. Hofer, J. Matias, U. Nierste, S. Pokorski, and J. Rosiek, Phys. Rev. D **92**, 054013 (2015); A. Crivellin, J. Fuentes-Martin, A. Greljo, and G. Isidori, Phys. Lett. B **766**, 77 (2017).

[6] K. Cheung, T. Nomura, and H. Okada, Phys. Rev. D **94**, 115024 (2016); R. Alonso, P. Cox, C. Han, and T. T. Yanagida, Phys. Lett. B **774**, 643 (2017).

[7] R. Aaij *et al.* (LHCb Collaboration), Phys. Rev. Lett. **113**, 151601 (2014).

[8] H. Fritzsch, Phys. Lett. **73B**, 317 (1978); P. Ramond, R. Roberts, and G. G. Ross, Nucl. Phys. **B406**, 19 (1993); G. Branco, D. Emmanuel-Costa, and R. Gonzalez Felipe, Phys. Lett. B **477**, 147 (2000); R. Roberts, A. Romanino, G. G. Ross, and L. Velasco-Sevilla, Nucl. Phys. **B615**, 358 (2001); H. Fritzsch and Z.-z. Xing, Phys. Lett. B **555**, 63 (2003); M. Gupta and G. Ahuja, Int. J. Mod. Phys. A **27**, 1230033 (2012).

[9] C. D. Froggatt and H. B. Nielsen, Nucl. Phys. **B147**, 277 (1979); S. F. King and G. G. Ross, Phys. Lett. B **520**, 243 (2001); **574**, 239 (2003); S. F. King, J. High Energy Phys. 08 (2005) 105; A. H. Galeana, R. E. Martinez, W. A. Ponce, and A. Zepeda, Phys. Rev. D **44**, 2166 (1991); A. Hernandez and R. Martinez, Phys. Rev. D **51**, 3962 (1995).

[10] F. Wilczek and A. Zee, Phys. Lett. **70B**, 418 (1977); E. Ma and G. Rajasekaran, Phys. Rev. D **64**, 113012 (2001); K. S. Babu, E. Ma, and J. W. F. Valle, Phys. Lett. B **552**, 207 (2003); E. Ma, Phys. Rev. D **70**, 031901 (2004); G. Altarelli and F. Feruglio, Nucl. Phys. **B741**, 215 (2006); S. L. Chen, M. Frigerio, and E. Ma, Nucl. Phys. **B724**, 423 (2005); A. Zee, Phys. Lett. B **630**, 58 (2005); P. D. Carr and P. H. Frampton, arXiv:hep-ph/0701034; F. Feruglio, C. Hagedorn,

Y. Lin, and L. Merlo, Nucl. Phys. **B775**, 120 (2007); M. C. Chen and K. T. Mahanthappa, Phys. Lett. B **652**, 34 (2007); P. H. Frampton and T. W. Kephart, J. High Energy Phys. 09 (2007) 110; A. Aranda, Phys. Rev. D **76**, 111301 (2007).N. Assad, B. Fornal, and B. Grinstein, Phys. Lett. B **777**, 324 (2018).

[11] J. L. Hewett and T. G. Rizzo, Phys. Rep. **183**, 193 (1989); A. E. Faraggi and D. V. Nanopoulos, Mod. Phys. Lett. A **06**, 61 (1991); P. Anastasopoulos, T. P. T. Dijkstra, E. Kiritsis, and A. N. Schellekens, Nucl. Phys. **B759**, 83 (2006); S. A. Abel, M. D. Goodsell, J. Jaeckel, V. V. Khoze, and A. Ringwald, J. High Energy Phys. 07 (2008) 124.

[12] R. Martinez, J. Nisperuza, F. Ochoa, and J. P. Rubio, Phys. Rev. D **89**, 056008 (2014).

[13] S. F. Mantilla, R. Martinez, and F. Ochoa, Phys. Rev. D **95**, 095037 (2017).

[14] S. F. Mantilla and R. Martinez, Phys. Rev. D **96**, 095027 (2017).

[15] P. Batra, B. A. Dobrescu, and D. Spivak, J. Math. Phys. **47**, 082301 (2006).

[16] R. Martinez, J. Nisperuza, F. Ochoa, and J. P. Rubio, Phys. Rev. D **90**, 095004 (2014).

[17] W. Grimus and L. Lavoura, J. High Energy Phys. 11 (2000) 042.

[18] G. Buchalla, A. J. Buras, and M. E. Lautenbacher, Rev. Mod. Phys. **68**, 1125 (1996); A. J. Buras, in *Probing the Standard Model of Particle Interactions*, edited by R. Gupta *et al.* (Elsevier Science B.V., Amsterdam, 1998), p. 281.

[19] G. Hiller and F. Kruger, Phys. Rev. D **69**, 074020 (2004).

[20] C.-W. Chiang, X.-G. He, and G. Valencia, Phys. Rev. D **93**, 074003 (2016).

[21] G. D'Amico, M. Nardecchia, P. Panci, F. Sannino, A. Strumia, R. Torre, and A. Urbano, J. High Energy Phys. 09 (2017) 010.

[22] M. Aaboud *et al.* (ATLAS Collaboration), J. High Energy Phys. 10 (2017) 182; A. M. Sirunyan *et al.* (CMS collaboration), Report No. CMS-PAS-EXO-16-031, 2016.

[23] C. Patrignani *et al.* (Particle Data Group), Chin. Phys. C **40**, 100001 (2016).